UNIVERSITAT POLITÈCNICA DE VALÈNCIA

PhD IN BIOTECHNOLOGY

A ROLE FOR PFD IN H2A.Z DEPOSITION IN ARABIDOPSIS

CRISTINA MARÍ CARMONA

ADVISORS:

Dr. MIGUEL ÁNGEL BLÁZQUEZRODRÍGUEZ

Dr. DAVID ALABADÍ DIEGO

VALENCIA, JANUARY 2021

Esta Tesis doctoral ha sido posible gracias al contrato de Formación de Personal Investigador ofrecido por la Universidad Politécnica de Valencia y a la financiación de Pedro J. Marí & Asociados. El proyecto al que pertenece este trabajo ha sido financiado por la Agencia Española de Investigación BIO2013-43184-P y BIO2016-79133-P.

SUMMARY

The prefoldin complex (PFDc) participates in cellular proteostasis in eukaryotes by acting as cochaperone of the chaperonin CTT. This role is mainly exerted in the cytoplasm where it contributes to the correct folding of client proteins, thus preventing them to form aggregations and cellular damage. Several reports indicate, however, that they also play a role in transcriptional regulation in the nucleus in several model species. In this work, we have investigated how extended is the role of PFDs in nuclear processes by inspecting their interactome and their coexpression networks in yeast, fly, and humans. The analysis indicates that they may perform extensive, conserved functions in nuclear processes. The construction of the predicted interactome for Arabidopsis PFDs, based on the ortholog interactions, has allowed us to identify many putative PFD interactors linking them to unanticipated processes, such as chromatin remodeling. Based on this analysis, we have investigated the role of PFDs in H2A.Z deposition through their interaction with the chromatin remodeling complex SWR1c. Our results show that PFDs have a positive effect on SWR1c, which is reflected in defects in H2A.Z deposition in hundreds of genes in seedlings defective in PFD3 and PFD5 activities.

RESUMEN

El complejo prefoldina (PFDc) participa en la proteostasis celular en eucariotas actuando como cochaperona de la chaperonina CTT. Este papel se ejerce principalmente en el citoplasma, donde contribuye al correcto plegamiento de las proteínas cliente, evitando así que se formen agregaciones y daño celular. Varios informes indican, sin embargo, que también juegan un papel en la regulación transcripcional en el núcleo en varias especies modelo. En este trabajo, hemos investigado cuán extendido es el papel de la PFD en los procesos nucleares al estudiar su interactoma y sus redes de coexpresión en levaduras, moscas y humanos. El análisis indica que pueden realizar una amplia y conservada variedad de funciones en procesos nucleares. La construcción del interactoma predicho para las PFD de Arabidopsis, basado en interacciones ortólogas, nos ha permitido identificar muchos putativos interactores de PFD que los vinculan a procesos no esperados, como la remodelación de la cromatina. Basados en este análisis, hemos investigado el papel de la PFD en la deposición de H2A.Z a través de su interacción con el complejo remodelador de la cromatina SWR1c. Nuestros resultados muestran que la PFD tienen un efecto positivo sobre SWR1c, lo que se refleja en defectos en la deposición de H2A.Z en cientos de genes en plántulas defectuosas en las actividades de PFD3 y PFD5.

RESUM

El complex prefoldina (PFDc) participa a la proteostasis cel·lular en eucariotes actuant com co-xaperona de la xaperonina CTT. Aquest paper s'exerceix principalment en el citoplasma, on contribueix al correcte plegament de les proteïnes client, evitant així que es formen agregacions i dany cel·lular. Diversos informes indiquen, però, que també juguen un paper en la regulació transcripcional en el nucli en diverses espècies model. En aquest treball, hem investigat com d'estès és el paper de la PFD en els processos nuclears estudiant el seu interactoma i les seues xarxes de coexpressió en llevats, mosques i humans. L'anàlisi indica que poden realitzar una àmplia i conservada varietat de funcions en processos nuclears. La construcció de l'interactoma predit per a les PFD d'Arabidopsis, basat en interaccions ortòlegs, ens ha permès identificar molts interactors putatius de les PFDs que les vinculen a processos no esperats, com és la remodelació de la cromatina. Amb base en aquest anàlisi, hem investigat el paper de la PFD en la deposició d'H2A.Z a través de la seva interacció amb el complex remodelador de la cromatina SWR1c. Els nostres resultats mostren que les PFDs tenen un efecte positiu sobre SWR1c, que es reflecteix en defectes en la deposició de H2A.Z en centenars de gens en plàntules defectuoses en les activitats de PFD3 i PFD5.

TABLE OF CONTENTS

INTRODUCTION

One of the most interesting aspects studied in plants is their high degree of developmental plasticity. They integrate environmental signals, like temperature and light, with endogenous signals such as nutrient levels and age, to establish specific gene expression patterns and therefore set the appropriate developmental and ambient response programs (Scheres & Van Der Putten, 2017).

The molecular mechanisms relaying the transduction of external and endogenous information into gene expression have not been completely described yet. Over the last 20 years, studies have shown that phytohormones control both developmental processes and adaptive responses, playing key roles in the coordination of signal transduction pathways and transcription regulation. Among these hormones, gibberellins (GAs) are known to modulate a wide variety of developmental and cellular processes that need to be precisely coordinated with the environment: cellular expansion and proliferation, seed dormancy and germination, photomorphogenesis, gravitropism, flowering, pollen maturation, biotic and abiotic stress responses (for complete review see Davière & Achard, 2016; Thomas et al., 2016). How are GAs able to regulate so many different processes?

DELLA regulate transcriptional programs through the interaction with multiple transcription factors

The GA signalling pathway relies on the activity of the DELLA proteins, nuclear-localized transcriptional regulators that repress GA responses. DELLA levels are regulated by GAs in such a way that in the absence of the hormone, DELLAs are accumulated in the nucleus and GA responses are repressed; when synthesized, binding of GA molecules to the GIBBERELLIN INSENSITIVE DWARF1 (GID1) receptor allows their interaction with the DELLA proteins, which are then ready for ubiquitination by SCF^{SLY1} E3 ligase and degradation by 26S proteasome, hence relieving the repression. When they are accumulated in the nucleus, DELLAs regulate gene transcription through physical interaction with multiple transcription factors and other transcriptional regulators (reviewed by Vera-Sirera et al., 2016).

Several studies have demonstrated the direct interaction of DELLA with a large number of proteins, and have uncovered three general molecular mechanisms of action so far: (i) as formerly found with PHYTOCHROME INTERACTING FACTOR3 (PIF3) and PIF4 (De Lucas et al., 2008; Feng et al., 2008), DELLA can sequester a transcription factor, directly inhibiting binding to the target DNA sequence and transcription; (ii) DELLA can also act as co-activators (Hernández-García et al., 2019; Marín-de la Rosa et al., 2015), binding transcription factors at the target loci and promoting transcriptional activation, as in the case of ARABIDOPSIS RESPONSE REGULATOR1 (ARR1), and (iii) DELLA can sequester transcriptional regulators that repress the activity of a transcription factor, indirectly facilitating its activity, as it has been shown for JAZ proteins (Hou et al., 2010; D. L. Yang et al., 2012).

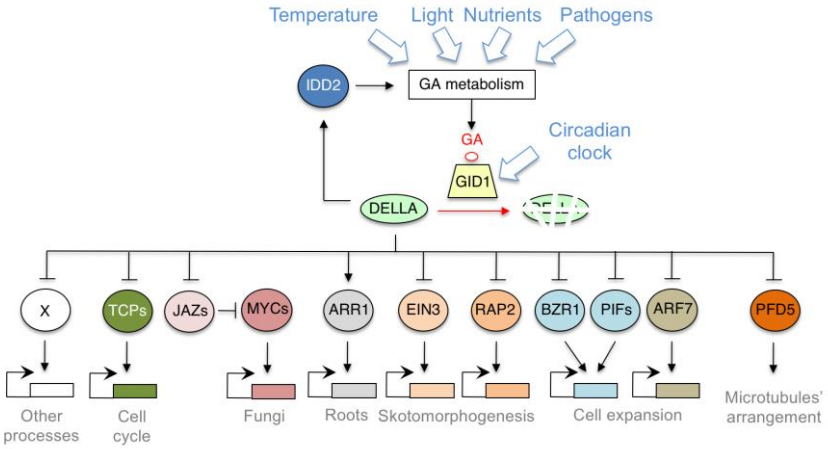

Figure 1. Simplified scheme of GA/DELLA function in the environmental modulation of cellular processes. DELLAs act as transcriptional hubs modifying the activity of different transcription factors (TFs). They also sequester PFD in the nucleus, thereby affecting microtubule organization. (Extracted from Thomas et al., 2016)

The observation that GA perception is regulated by the circadian clock (Arana et al., 2011), and GA metabolism is very sensitive to light, temperature and osmotic stress (reviewed by Colebrook et al., 2014; Hedden & Thomas, 2012) ultimately results in a tight regulation of DELLA protein levels by

environmental cues. In addition to this, DELLAs have the ability to interact with diverse classes of transcriptional regulators -many of them core components of other hormone signalling pathways-, suggesting that they act as hubs in growth and ambient response regulatory networks (Claeys et al., 2014; Davière & Achard, 2016; Marín-de La Rosa et al., 2014). Therefore, it has been proposed that one important function of DELLA is to transduce environmental information to cellular processes, mostly through transcriptional modulation. (Figure 1)

Interestingly, some evidences indicate that DELLA proteins act through other mechanisms not involving bona fide transcription factors to regulate physiological processes. Locascio et al. (2013) identified two atypical interactors, PREFOLDIN5 (PFD5) and PFD3 -which are part of the prefoldin complex-, showing for the first time that DELLAs can control non-transcriptional responses (see below).

The Prefoldin complex

Prefoldin is a heterohexameric complex (PFDc) composed of two α-class subunits (PFD3 and 5) and four β-class subunits (PFD1, 2, 4 and 6), forming a characteristic jellyfish-like structure with a double β-barrel hexamer and six coiled coils emerging from it (Figure 2) (Leroux, 1999; Siegert et al., 2000). Originated in archaea, it is conserved in eukaryotes, where it was first identified as a co-chaperone, delivering partially folded or unfolded substrates to class II chaperones (Bogumil et al., 2013; Vainberg et al., 1998).

In archaea, prefoldin plays a general role as chaperone, being able to stabilize and assist the folding of a wide range of proteins (Lim et al., 2018); however, in eukaryotes it shows high substrate specificity. Although it has been demonstrated that eukaryotic PFD prevents the aggregation of some proteins (Abe et al., 2013; Sörgjerd et al., 2013; Takano et al., 2014; Tashiro et al., 2013), it delivers nascent polypeptides of actin, α- and β-tubulin to Chaperonin Containing Tailless complex polypeptide 1 (CCT), a molecular chaperone assisting the assembly of actin filaments and microtubules, as shown by Geissler et al. (1998) and Vainberg et al. (1998) (Figure 2). These pioneering studies revealed that *Saccharomyces cerevisiae* prefoldin mutants have cytoskeletal defects and low levels of tubulin; later investigations by Lacefield

et al. (2006) demonstrated that, in yeast, the availability of α/β-tubulin heterodimers is key for microtubules to reach a proper length and organize correctly, and that PFDc activity is essential for this. Cytoskeleton abnormalities and altered tubulin levels have also been reported for *Caenorhabditis elegans*, *Drosophila melanogaster* and mouse prefoldin mutants (Cao et al., 2008; Delgehyr et al., 2012; Lee et al., 2011; Lundin et al., 2008), indicating that this specific role of prefoldin is conserved amongst eukaryotes.

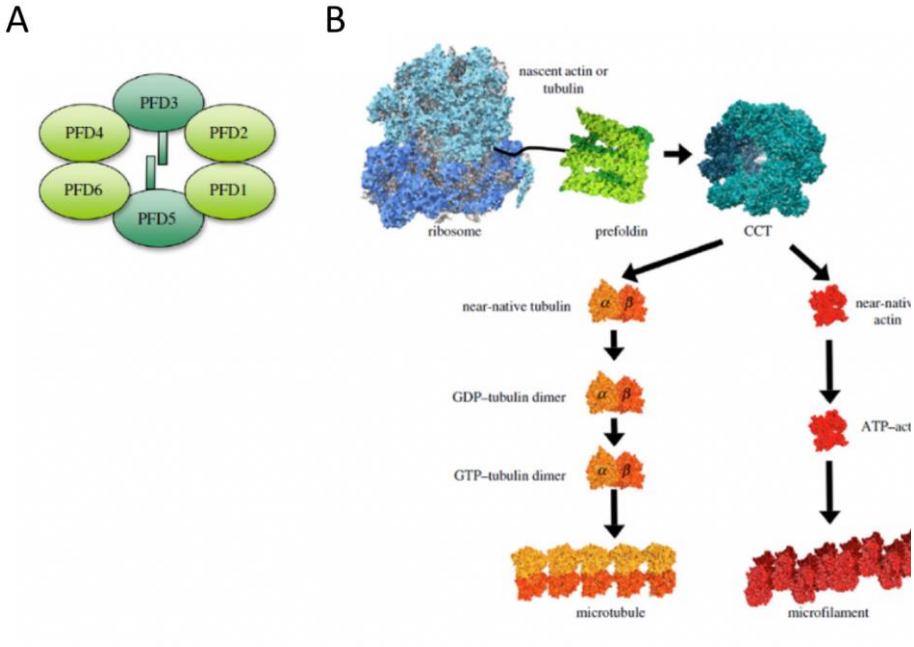

Figure 2. The PFD complex. (A) Scheme of the subunits' arrangement. (B) Role as a co-chaperone in the folding of at least tubulin and actin polypeptides (image adapted from Millán-Zambrano & Chávez, 2014)

Consistent with this, *Arabidopsis thaliana* PFD3, PFD4, PFD5 and PFD6 have been found to be necessary to reach adequate tubulin levels and for microtubule dynamics and organization (Gu et al., 2008; Perea-Resa et al., 2017; Rodríguez-Milla and Salinas, 2009). Further proof of the conserved function of the PFDc as co-chaperone for actin and tubulin folding is the complementation of yeast prefoldin mutants by the corresponding human, mouse and plant genes (Geissler et al., 1998; Rodríguez-Milla and Salinas, 2009). Recent results by Gestaut et al. (2019) indicate that PFDc acts

remodelling actin molecules already bound to CCT but presenting a wrong conformation, thus minimizing aggregation and increasing the folding kinetics. So, PFDc not only delivers substrates to CCT prior to folding, but also receives substrates from CCT during the folding, enhancing its processivity.

Prefoldin localizes in the nucleus

The function as co-chaperones folding tubulins and actin takes place in the cytoplasm, but research by Locascio et al. (2013) demonstrated the DELLAs interact with PFD in the nucleus in *Arabidopsis*. In particular, authors showed that PFDs preferably accumulate in the nucleus when DELLA levels are high, while are mainly localized in the cytoplasm when DELLA levels are low. Importantly, the presence of PFDs in the nucleus impairs their role in the cytoplasm, i.e. tubulins are not properly folded, resulting in lower tubulin levels and defective microtubules arrangement, subsequently preventing anisotropic cell growth (Figure 3).

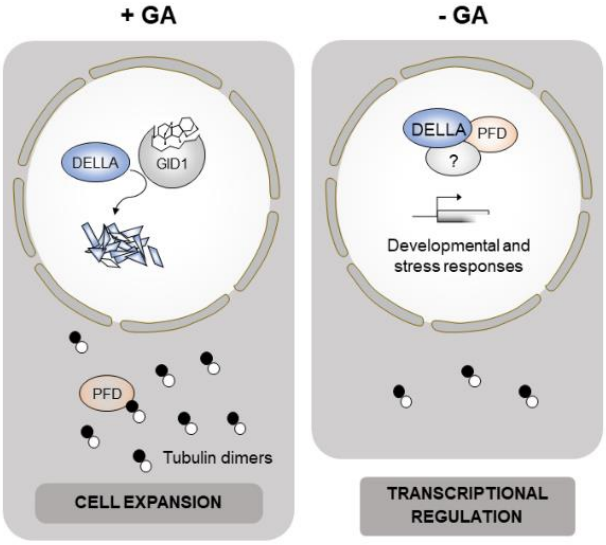

Figure 3. GA-dependent accumulation of PFDc in the nucleus. Under low GA levels, DELLA proteins sequester PFDc away from the compartment where they are required for the correct folding of tubulin. This results in the reduction of a/b-tubulin heterodimers and microtubule disarrangement, but it might also facilitate hypothetical functions of PFD in the nucleus.

The localization of PFD in the nucleus raises the interesting question of whether this is just a sequestering mechanism to prevent PFD cytoplasmic functions, or PFD performs an active role in the nucleus. Indeed, information reported in the literature indicates that PFD (as a whole or the individual subunits) participates in regulating different steps of transcription (for a complete review on the subject, see Payán-Bravo et al., 2018).

Nuclear roles of prefoldin

The first evidence showing a role for a particular PFD in transcription was the regulation of the activity of the c-Myc TF by PFD5 subunit in humans. The direct interaction of PFD5 with one of the c-Myc transactivation domains represses its transcriptional activity (Hagio et al., 2006; Mori et al., 1998; Satou et al., 2001; Watanabe et al., 2002) and may also promote its degradation (Kimura et al., 2007; Narita et al., 2012). In addition to PFD5, PFD3 subunit has been shown to interact with the viral HBx protein and the TF NF-κB, upregulating the transactivation activity of NF-κB (S. Y. Kim et al., 2008). The regulation of TFs by PFDs seems to be conserved in eukaryotes, since the DELLA-dependent accumulation of PFD4 in the nucleus allows its interaction with the TF HY5 under cold conditions, promoting its degradation and the transcriptional downregulation of anthocyanins biosynthesis genes in *Arabidopsis* (Perea-Resa et al., 2017). Another example of transcriptional regulation was published by Yamane et al. (2015), who studying the infertility phenotype of PFD5 mutant mice, found out that this subunit binds promoter and genic regions of different spermatogenesis-related genes, regulating them at the transcriptional level, most likely through interaction with TFs. Similarly, Yoshida et al. (2008) reported the binding of human PFD5 to the promoter of *wnt4* gene and its downregulation, and Wang et al. (2017) demonstrated that human PFD1 promotes epithelial-mesenchymal transition induction and metastasis of lung cancer cells by binding at the promoter of cyclin A and supressing its expression.

The role of PFDs in the nucleus is not only related to the activity of TFs. Recent results from our lab indicate that PFDs affect other stages of gene transcription in *Arabidopsis*, such as pre-mRNA splicing (Esteve-Bruna et al.,

2020). In yeast, PFD subunits 1, 2, 5 and 6 have been shown to be recruited to chromatin in a transcription-dependent manner. Evidences indicate that prefoldin is required to aid RNA polymerase II during transcription elongation of long genes and genes with a canonical TATA box by preventing the polymerase arrest. It has been proposed that, to do so, yeast prefoldin contributes to chromatin dynamics, probably in histone eviction during transcription elongation (Millán-Zambrano et al., 2013).

Indeed, results obtained by an *in silico* analyses performed in the first section of this Thesis, suggest that PFDc is implicated in chromatin dynamics.

Chromatin dynamics and the histone variant H2A.Z

In eukaryotic cells, DNA is packaged into chromatin in the nucleus. The basic repeating unit of chromatin is the nucleosome, 147 bp of DNA wrapped around an octamer formed by two copies of each of the canonical histones H2A, H2B, H3 and H4, where a tetramer of $(H3\text{-}H4)_2$ in the inner region is flanked by two dimers of H2A-H2B positioned in the surface (Luger et al., 1997). Nucleosomes create a compact structure that blocks the access of transcription factors and machineries involved in DNA processes, hence the importance of chromatin dynamics in the regulation of gene expression patterns, DNA repair, replication and recombination.

Cells have developed at least three mechanisms of chromatin dynamics and remodelling: DNA modifications and histone post-translational modifications (PTMs), sliding of nucleosomes along the DNA, and the exchange of canonical histones by histone variants (Talbert & Henikoff, 2010). Histone variants differ from canonical histones in the amino acid sequence, which gives them different biophysical properties that alter nucleosome structure and characteristics, and also because their expression and incorporation to the genome are not restricted to the S phase (Malik & Henikoff, 2003; Biterge & Schneider, 2014). Replication-independent deposition makes them suitable to mediate responses to environmental cues, happening throughout the cell cycle (Talbert & Henikoff, 2014).

H2A.Z is the most evolutionarily conserved H2A variant, and has been identified in numerous eukaryotes (van Daal et al., 1990; Thatcher and

Gorovsky, 1994; Malik and Henikoff, 2003). Phylogenetic analyses show that H2A.Z diverged early in eukaryotic evolution and has remained highly conserved ever since. Actually, there is around 90% amino acid identity in H2A.Z variants between species and only about 60% identity between H2A.Z and H2A within the same organism.

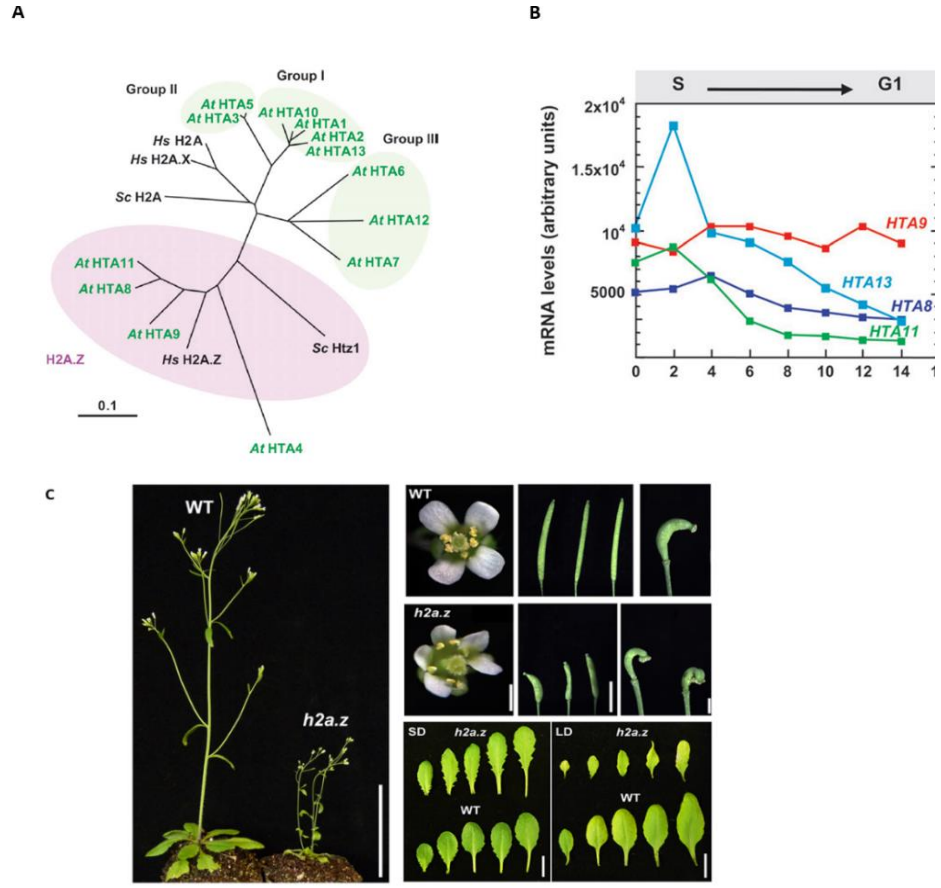

Figure 4. Conservation of H2A.Z and functional redundancy in *Arabidopsis*. (A) Phylogenetic relationships between H2A paralogues (HTA1 to 13), which classified into 4 groups. Group 4 (pink) contains H2A.Z variants. *At*, *A. thaliana*, *Hs*, *Homo sapiens*; *Sc*, *S. cerevisiae*. (B) mRNA levels of H2A.Z genes (HTA8, HTA9, HTA11) and a canonical H2A gene (HTA 13) at different time points of cell cycle, from the beginning of S phase until G1. Expression of HTA9 is independent of the cell cycle. (C) Phenotype of the *Arabidopsis* triple *h2az* mutant showing pleiotropic defects all along development. (Extracted from Coleman-Derr & Zilberman, 2012; March-Díaz & Reyes, 2009)

Arabidopsis contains three genes coding for H2A.Z histones: *HTA8*, *HTA9* and *HTA11* (Yi et al., 2006). All of them show the same tissue expression pattern, and their respective single mutants do not display any apparent phenotypic difference, which suggests a high degree of functional redundancy (Choi et al., 2007; March-Díaz et al., 2008). However, the *hta9 hta11* double mutant plants present pleiotropic defects, with serrated leaves and elongated petioles, reduced apical dominance, shorter internodes, small flowers – sometimes with one or more extra petals and sepals, short stamens, short and thickened siliques, and early flowering. This result indicates that *HTA8* cannot fully compensate for the loss of *HTA9* and *HTA11*. This may be due to the low expression levels of *HTA8*. The triple *hta8 hta9 hta11* mutant (or *h2az* mutant) is still viable but severely affected (Coleman-Derr & Zilberman, 2012).

H2A.Z deposition. The SWR1 complex

H2A.Z dynamics is regulated by different ATP-dependent chromatin-remodelling complexes that control the deposition and removal of the histone: the SWI2/SNF2-RELATED1 complex (SWR1c) and the INOSITOL-REQUIRING80 (INO80) complex, respectively (Gerhold & Gasser, 2014). The yeast SWR1c was the first one described to be involved in H2A.Z dynamics. The catalytic subunit of the complex is Swr1 (Kobor et al., 2004; Krogan et al., 2003; Mizuguchi et al., 2004), an ATPase of the INO80 family that interacts with 13 other proteins to form a complex that mediates H2A.Z deposition by evicting H2A/H2B dimers in the nucleosomes and incorporating H2A.Z/H2B dimers (Wu et al., 2005, 2009). The experiments performed by Wu et al. (2005, 2009) and the electron microscopy data by Nguyen et al. (2013) show that the SWR1c is composed of three modules assembled on the core subunit Swr1 (Figure 5): a heterohexameric ring of RuvB-LIKE PROTEIN1/2 (Rvb1/Rvb2) subunits (AAA+ ATPases), which together with the catalytic subunit Swr1, brackets two independently assembled multisubunit modules, the N-module and the C-module.

The composition of the SWR1c has been widely studied in yeast, and it is largely conserved among eukaryotes, including *Arabidopsis* (Table 1). In yeast,

the N-module comprises subunits Bdf1, Arp4, Act1, Swc4, Yaf9 and Swc7; some of them show affinity for canonical histones and acetylated histone tails, which implies that this module participates in nucleosome binding and in targeting the complex to particular locations in the chromatin. The C-module is formed by subunits Swc3, Swc2, Arp6 and Swc6; this module binds H2A.Z/H2B free dimers and loads them into the complex. Interestingly, four subunits of the SWR1c (Yaf9, Swc4, Arp4 and Act1, see Table 1) are also part of the NuA4 complex, a histone acetyltransferase (HAT) for histones H4, H2A and H2A.Z (Billon & Côté, 2012; Lu et al., 2009). It is worth noticing that acetylation of H4 and H2A by NuA4c promotes the deposition of H2A.Z by SWR1c (Altaf et al., 2010), and once in the nucleosomes, H2A.Z can be acetylated by NuA4c (Keogh et al., 2006).

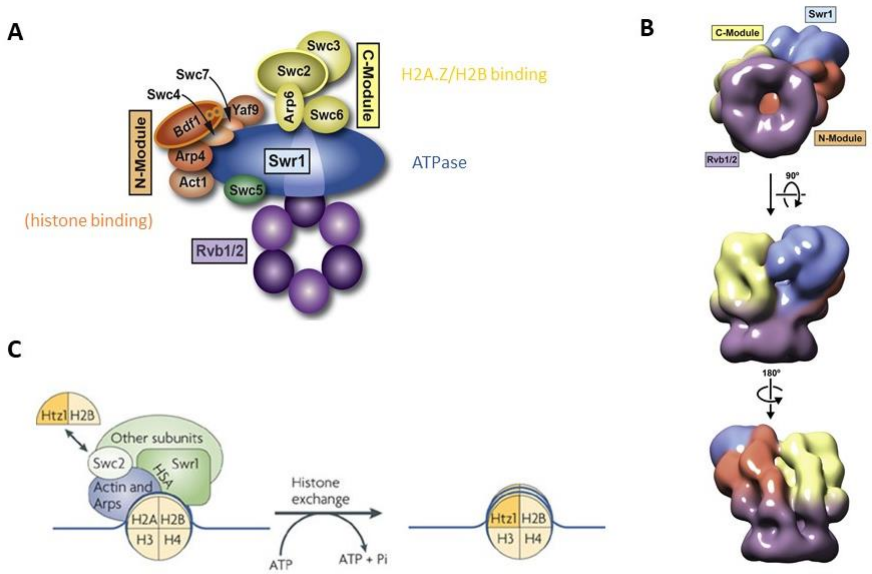

Figure 5. Structure and function of the yeast SWR1 complex. (A) Model of the yeast SWR1c composition. (B) Different views of the 3D structure of the complex. (C) ATP-dependent exchange of H2A by H2A.Z catalyzed by the SWR1 complex. (Extracted from Nguyen et al., 2013)

The INO80 chromatin remodelling complex is also involved in H2A.Z dynamics. Yeast INO80c can regulate the genome-wide distribution of H2A.Z by removing this histone variant from promoters during transcriptional induction (Kapoor & Shen, 2014; Papamichos-Chronakis et al., 2011). This complex also shares four subunits with the SWR1c: Arp4, Act1, Rvb1 and Rvb2 (Billon & Côté, 2012; Shen et al., 2000).

Genetic analyses in *Arabidopsis* identified several homologs of the SWR1c owing to the early flowering phenotype of some of their mutants. For instance, PHOTOPERIOD-INDEPENDENT EARLY FLOWERING 1 (PIE1, homologous to the ATPase subunit), ACTIN-RELATED PROTEIN 6 (ARP6), SWR1 COMPLEX SUBUNIT6 (SWC6), and ARP4 have been studied at a genetic and molecular level (Choi et al., 2005, 2007; Deal, 2005; Deal et al., 2007; Lázaro et al., 2008; March-Díaz et al., 2008; Martin-Trillo et al., 2006; Noh & Amasino, 2003). Loss-of-function mutants of these subunits showed similar morphological and developmental phenotypic defects to those found in the *hta9hta11* mutant, though with different severity levels. In addition, these studies showed physical interaction between subunits and defects in H2A.Z deposition in mutant plants, strongly supporting the existence of a conserved SWR1c in plants. A homology analysis by March-Díaz & Reyes (2009) identified all the putative subunits of the complex in *Arabidopsis*, but it has only been recently that the composition of the AtSWR1c has been confirmed by four independent laboratories with affinity purification approaches (Gómez-Zambrano et al., 2018; Luo et al., 2020; Potok et al., 2019; Sijacic et al., 2019) (Table 2).

According to the current model of SWR1c in plants, several subunits are conserved, for instance, the catalytic subunit, the Rvb1/Rvb2 ring, the C-module (except for the Swc3 subunit that does not have a plant homolog), and subunits Arp4, Swc4, Yaf9 and Act1 of the N-module. However, the putative Swc5 ortholog in plants has not been co-precipitated with SWR1c subunits in any experiment. Interestingly, three putative new plant-specific subunits have been consistently found in these experiments – METHYL-CpG-BINDING DOMAIN PROTEIN (MBD9), TRANSCRIPTION-ASSOCIATED PROTEIN1A (TRA1a) and TRA1b– although further studies are required to determine whether they are functional components of the plant SWR1c.

Table 1. Composition of *S. cerevisiae* SWR1 complex and its counterparts in *H. sapiens* and *D. melanogaster*, and homologs in *A.thaliana*. Homolog proteins are shown in the same line. Notice the overlap with INO80 and NuA4 complexes, involved in H2A.Z eviction/deposition and H2A.Z modification, respectively. Table assembled according to (Altaf et al., 2010; Giaimo et al., 2019; March-Díaz & Reyes, 2009; Morrison & Shen, 2009; Nguyen et al., 2013)

Yeast			Human		Fly	*Arabidopsis*
NuA4	**SWR1**	**INO80**	**SRCAP**	**Ep400/Tip60**	**DOMINO**	**SWR1**
	Swr1		SRCAP	Ep400	DOM-B	PIE1
		Ino80				
Eaf1						
Esa1				Tip60		
	Rvb1	Rvb1	Tip49a	Tip49a	PONT	RVB1
	Rvb2	Rvb2	Tip49b	Tip49b	REPT	RVB2A RVB2B
Arp4	Arp4	Arp4	BAF53a	BAF53a	BAP55	ARP4
	Arp6		ARP6		ARP6	ARP6
Yaf9	Yaf9		GAS41	GAS41	GAS41	YAF9A YAF9B
	Swc2		YL1	YL1	YL1	SWC2
	Swc3					
Eaf2	Swc4		DMAP1	DMAP1	DMAP1	SWC4
	Swc5					
	Swc6		Znf-HIT1			SWC6
	Swc7					
Act1	Act1	Act1		Actin		ACT1
	Bdf1		BRD8	BRD8	BRD8	
Tra1				TRRAP		
Epl1			EPC-like			
			EPC1			
Yng2				ING3		
Eaf3				MRG15	MRG15	
				MRGX		
Eaf5						
Eaf6				FLJ11730		
Eaf7				MRGBP	MRGBP	
					PPS	
					HCF	
		Arp5				
		Arp8				
		Taf14				
		Ies1				
		Ies2				
		Ies3				
		Ies4				
		Ies5				
		Ies6				
		Nhp10				

Table 2. Identity of the genes encoding SWR1c subunits in *A. thaliana*. Table assembled according to (Gómez-Zambrano et al., 2018; Luo et al., 2020; Potok et al., 2019; Sijacic et al., 2019)

S. cerevisiae	A. thaliana	Locus
Swr1	PIE1	At3g12810
Rvb1	RVB1	At5g22330
Rvb2	RVB2A	At5g67630
Yaf9	YAF9A	At5g45600
Arp4	ARP4	At1g18450
Arp6	ARP6	At3g33520
Swc2	SWC2	At2g36740
Swc3		
Swc4	SWC4	At2g47210
Swc5		
Swc6	SWC6	At5g37055
Swc7		
Act1	ACT1	At2g37620
Bdf1		
	MBD9	AT3G01460
	TRA1A	AT2G17930
	TRA1B	AT4G36080

Molecular functions of H2A.Z

The high degree of conservation of H2A.Z throughout evolution indicates that it performs essential functions. Accordingly, loss of H2A.Z in metazoans causes lethality, while H2A.Z-deficient yeasts are viable but show severe growth reduction (Faast et al., 2001; Jackson & Gorovsky, 2000; Liu & Gorovsky, 1996; Van Daal & Elgin, 1992). The *Arabidopsis h2az* mutant, though severely affected, is still viable (this is most likely because it is not a true null, since the *hta9* allele is a knock-down with transcript levels being ≈26% of the WT) (Coleman-Derr & Zilberman, 2012).

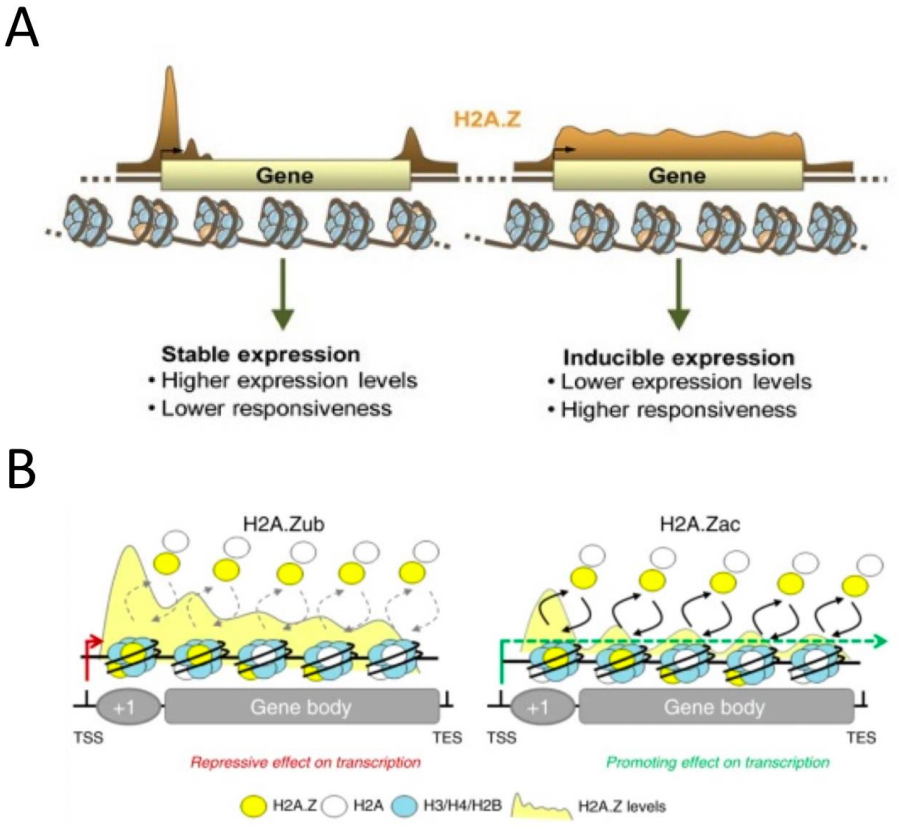

Figure 6. Hypothetical models for the regulation of gene expression by H2A.Z deposition. (A) Model proposed by the Zilberman Lab. (B) Currently accepted model (taken from Gómez-Zambrano et al., 2019).

Several reports have shown conserved molecular functions for H2A.Z in DNA damage repair and homologous recombination, heterochromatin regulation, maintenance of chromosome integrity and transcriptional regulation (Billon & Côté, 2012; Giaimo et al., 2019; Jarillo & Piñeiro, 2015; Marques et al., 2010).

In *Arabidopsis,* H2A.Z is known to regulate transcriptional responses to environmental cues, such as temperature changes, nutrient levels, pathogens and drought (Berriri et al., 2016; Kumar & Wigge, 2010; March-Díaz et al., 2008; Smith et al., 2010; Sura et al., 2017). As in other organisms, H2A.Z is mainly localised at the 5' end of genes, at the +1 nucleosome near the

transcription start site (TSS, Barski et al., 2007; Guillemette et al., 2005; Zhang & Pugh, 2011; Zilberman et al., 2008), but is also found at the 3' end of genes, gene bodies (Coleman-Derr & Zilberman, 2012; Dai et al., 2017a; Sura et al., 2017) and enhancers (Dai et al., 2017a; Subramanian et al., 2015).

The role of this variant in transcription is not completely understood yet, since multiple reports in yeast, animals and plants have shown both promoting and repressive effects. Studies by Zilberman et al. (2012) and Sura et al. (2017) showed different roles for H2A.Z depending on its location (Figure 6): they found that H2A.Z occupancy in the gene body is negatively correlated with transcription levels, and positively correlated with gene responsiveness –the degree to which a gene is differentially expressed among different conditions or tissue types; however, when H2A.Z is present in the +1 nucleosome it promotes transcription for some genes, in particular, highly and constitutively expressed genes.

In contrast to these reports, Dai et al. (2017) detected that H2A.Z at the +1 nucleosome is required to repress expression. Several studies in yeast and human indicate that H2A.Z postranslational modifications (PTMs) –specifically acetylation and ubiquitination– are key determining its role in transcription regulation. In *Arabidopsis,* there is evidence that H2A.Z acetylation at the +1 nucleosome is required for the activation of *FLOWERING LOCUS C* (*FLC*) expression (Crevillén et al., 2019). In addition, a recent report demonstrated that H2A.Z monoubiquitination is required for transcription repression by this histone in plants, instead of certain occupancy levels, suggesting that the different H2A.Z levels in activated and repressed genes found in previous studies are a direct consequence of the transcriptional activity (Gómez-Zambrano et al., 2019).

OBJECTIVES

As explained in the Introduction, we have accumulated evidence that points to a possible nuclear role of PFD, different to their well-studied function as co-chaperones for actin and tubulin folding:

(i) The conditional localization of PFD in the nucleus in *Arabidopsis*, as well as its reported presence in the nucleus of yeast cells.

(ii) The phenotype of *pfd* mutants in yeast and animals, part of which cannot be explained only by its cytosolic function as co-chaperone.

(iii) The reported physical interaction between some PFD subunits and transcription factors in animal cells.

(iv) The transcriptional defects caused by loss of PFD function in plant, yeast and animal cells.

In order to consolidate this view and obtain some insight on the possible nuclear role of PFD in the regulation of gene expression in plants, we propose the following specific objectives:

1. **To determine the conservation of the nuclear interactome of PFD in yeast, animals and plants.** We will take advantage of the wealth of datasets publicly available for physical and genetic interactions for the *S. cerevisiae*, *D. melanogaster* and *A. thaliana* proteomes, as well as gene co-expression networks.
2. **To study in *Arabidopsis* the functional relevance of the physical interaction between PFD and the chromatin-remodeling SWR1 complex**, involved in H2A.Z deposition. We will systematically study physical interactions between the different PFDc and SWR1c subunits, and then analyze the consequences of the loss of PFD activity for SWR1c function.

MATERIALS AND METHODS

In silico analysis

Protein-protein and genetic interaction data were retrieved from BioGrid (https://thebiogrid.org/), IntAct (https://www.ebi.ac.uk/intact/) and MINT (https://mint.bio.uniroma2.it/) databases. Co-expression and Gene Ontology (GO) annotation data were retrieved from InterMine (http://intermine.org/), YeastNet v3 (https://www.inetbio.org/yeastnet/, Kim et al., 2014) and the Drosophila Gene Expression Tool (DGET, http://www.flyrnai.org/tools/dget/web, Hu et al., 2017). Additionally, a list of yeast chaperone interactors was obtained from Gong et al. (2009). *Arabidopsis* predicted interactome was obtained from Geisler-Lee et al. (2007). Networks were depicted with Cytoscape software (Shannon et al., 2003).

The heatmap integrating physical and genetic interactions in *S. cerevisiae* was elaborated classifying interactors in 4 categories: (1) no interaction, (2) genetic interaction, (3) physic interaction, (4) physic and genetic interaction. Genes with at least 1 physical interaction and 1 genetic interaction with one PFD subunit are included. The darker the colour, the more evidence of interaction.

Plant material and growth conditions

All plant lines were in Col-0 background. We used previously characterized T-DNA insertion lines: *arp6* (WiscDSLox_289_292L8; Martin-Trillo et al., 2006), *swc6-1* (SAIL_1142_C03; Lázaro et al., 2008), *h2az* (Coleman-Derr & Zilberman, 2012), *pfd3* and *pfd5* (GK-863G01 and GK-942H12-032877, respectively; Rodríguez-Milla & Salinas, 2009). The *pfd3 pfd5* and *pfd3 swc6-1* mutants were generated from genetic crosses of the respective single mutant lines. Seeds were sown on ½ MS medium (Duchefa), 0.8% (w/v) agar (pH 5.7) and stratified at 4 ºC in the dark for 4 days. Unless otherwise stated, plants were grown on MS plates for 2 weeks under short-day photoperiod (8h light/16 h dark), with light intensity of 100 µmol m^{-2} s^{-1}, at 22 ºC.

Flowering time analysis

Plants were germinated on MS plates at 22 ºC under short-day conditions. After 7 days, seedlings were transferred to soil and moved into growth

chambers at 16, 22 or 27 ºC. Flowering time was determined by counting the total number of leaves produced before the first flower.

Yeast two-hybrid assays

The coding sequence (CDS) of PFD subunits, SWR1c subunits, HTA8, HTA9 and HTA11 were transferred to both pGADT7 and pGBKT7 plasmids (Clontech) by Gateway technology. Haploid yeast strains Y2HGold and Y187 (Clontech) were transformed with pGBKT7 and pGADT7 constructs respectively, following the Lithium-Acetate method. Diploid cells carrying both plasmids were generated by mating and interaction assays were performed on synthetic complete minimal medium without His, Leu, and Trp, supplemented with 0–5 mM of 3-amino- 1,2,4-triazole (3-AT).

Protein co-immunoprecipitation assays

PFD6 CDS was transferred to pEarleyGate 104 vector and ARP6 CDS was transferred to pEarleyGate 203 vector. Constructs were introduced into *Agrobacterium tumefaciens* C58, and used to infiltrate *Nicotiana benthamiana* leaves, in combination and individually. The final optical density (OD_{600nm}) of each infiltrated culture was 0.1. Leaf samples were collected after 3 days. Frozen ground tissue was homogenized with extraction buffer (50mM Tris-HCl pH7, 10% glycerol, 1mM EDTA pH 8.0, 150 mM NaCl, 10mM DTT and 1X protease inhibitor cocktail [cOmplete EDTA free, Roche]) in a ratio 2:1 (v/v), and incubated on ice for 15 min. Extracts were centrifuged twice for 2 min at 14000 rpm at 4 ºC, and proteins were quantified by Bradford assay. 50 μg of total proteins were denatured in Laemmli buffer as an input sample. 1.5 mg of total proteins were incubated with 50 μL of anti-GFP paramagnetic beads (Miltenyi) for 2h at 4 ºC in a rotating wheel, and then loaded onto μcolumns (Miltenyi). Columns were washed with cold extraction buffer and proteins were eluted with Laemmli 1X, following manufacturer's instructions. Input and immunoprecipitated samples were analysed by Western blot.

Size exclusion chromatography assays

Extracts of wild-type and pfd3,5 seedlings were prepared in extraction buffer (50 mM Tris-HCl pH 7.5, 150 mM NaCl, 10 mM MgCl2, 10% Glycerol, 0.5% Nonidet P-40, 2 mM PMSF and 1X protease-inhibitor cocktail). Proteins were loaded in a SuperoseTM 6 Increase (GE Healthcare) column. Fourteen fractions (250 µL each) were collected and those where ARP6 is present are shown. Proteins in fractions were precipitated in 10% trichloroacetic acid on ice for 90 min and then washed twice with cold acetone before Western-blot analysis.

Subcellular fractionation assays

Subcellular fractionation was performed according to Zhang et al. (2014), with minor modifications. 1.5 grams of seedlings were ground in liquid nitrogen and homogenized in 3 mL of cold Honda buffer (0.44 M Sucrose, 20 mM HEPES KOH pH 7.4, 2.5% Percoll, 5% Dextran T40, 10 mM $MgCl_2$, 0.5% Triton X-100, 5mM DTT, 1 mM PMSF, and 1x protease inhibitor cocktail [cOmplete, EDTA-free; Roche]). The homogenate was filtered through two layers of Miracloth and centrifuged at 2000 g at 4 ºC for 5 min. 1 mL of the supernatant was centrifuged at 10000g at 4 ºC for 10 min, and collected as cytoplasmic fraction. The pellet was resuspended in 1 mL of Honda buffer and centrifuged at 1800g for 5 min to pellet the nuclei. Pellet was washed 4 times with Honda buffer, rinsed with 1X PBS buffer (137 mM NaCl, 2.7 mM KCl, 10 mM Na_2HPO_4, 2 mM KH_2PO_4) with 1mM EDTA, and resuspended with 150 µL of cold glycerol buffer (20 mM Tris-HCl pH 7.9, 50% glycerol, 75 mM NaCl, 0.5 mM EDTA, 0.85 mM DTT, 0.125 mM PMSF, and 1x protease inhibitor cocktail [cOmplete, EDTA-free; Roche]), to which 150 µL of cold nuclei lysis buffer was added (10 mM HEPES KOH pH 7.4, 7.5 mM MgCl2, 0.2 mM EDTA, 0.3 M NaCl, 1 M urea, 1% NP-40, 1 mM DTT, 0.5 mM PMSF, 10 mM β-mercaptoethanol, and 1x protease inhibitor cocktail [cOmplete, EDTA-free; Roche]). This was vortexed twice for 2 s and incubated on ice for 2 min, following centrifugation at 14000 rpm at 4 ºC for 2 min. The supernatant was collected as nucleoplasmic fraction. The chromatin pellet was rinsed with 1X PBS/1mM EDTA and resuspended in 150 µL cold glycerol buffer and 150 µL cold nuclei lysis buffer. Protein

concentrations were determined by using the Pierce 660 nm protein assay (Thermo-Fisher Scientific) according to the manufacturer´s instructions. The fractions were analysed by Western blot.

Western blot

Protein samples were separated by SDS-PAGE, transferred to PVDF membranes and immunolabeled with specific antibodies against anti-myc (1:1000, E910, Roche), anti-GFP (1:10000, Living Colors JL-8), anti-ARP6 (1:200, Kerafast EGA929), anti-DET3 (1:10000, provided by Karin Schumacher), or anti-H3 (1:5000, abcam ab1791). horseradish peroxidase-conjugated anti-rabbit (Agrisera) and anti-mouse (Agrisera) were used as secondary antibodies at 1/20,000 and 1/10,000 dilutions, respectively. Chemiluminiscence detection was performed with the Supersignal west FEMTO maximum sensitivity substrate (Thermo-Fisher Scientific) and protein bands were detected using the LAS-3000 Imaging system (Fujifilm). Protein bands were quantified with NIH ImageJ software (Rueden et al., 2017) for subcellular fractionation analysis.

RNA-seq and RNA-seq data analysis

Total RNA was extracted from Col-0, *arp6-1, swc6-1* and *pfd3 pfd5* seedlings (three biological replicates) using RNeasy Plant Mini Kit (Qiagen) according to the manufacturer´s instructions. The RNA concentration and integrity [RNA integrity number (RIN)] were measured in an RNA nanochip (Bioanalyzer, Agilent Technologies 2100) by the IBMCP Genomics Service. Library preparation and sequencing were performed by the Genomics Service of the University of Valencia. Reads were mapped to the *Arabidopsis thaliana* TAIR10 reference genome using Bowtie 2 (Langmead & Salzberg, 2012), and counts were calculated with HTSeq-count software (Anders et al., 2015) and differentially expressed genes (DEG) were identified with edgeR Bioconductor package (McCarthy et al., 2012). DEGs were selected according to a fold change cut-off $>|1.5|$ and a p value <0.05. Normalized expression values for each gene were calculated as transcripts per kilobase million (TPM). Heatmap representation was generated with Pheatmap R package (Kolde, 2015). GO annotation and over-representation of biological

processes (BP) terms were performed with the clusterProfiler Bioconductor package (Yu et al., 2012) using p-value and q-value cut-offs of 0.01. Redundancy of enriched GO terms was reduced and results were represented in a figure using GOSemSim Bioconductor package (Yu et al., 2010), with similarity cut-off of 0.7 on level 3 GO terms.

ChIP experiments

Chromatin was extracted and immunoprecipitated from Col-0, *swc6-1* and *pfd3,pfd5* seedlings (two biological replicates) as described in in (Gallego-Bartolomé et al., 2019), using anti-HTA9 (10 μg, Agrisera AS10 718) and anti-H2B (3μg, abcam ab1790). For ChIP-seq, library preparation and sequencing were carried out by the CRG Genomics Core Facility (Barcelona, Spain). For ChIP-qPCR, amplification was performed using 7500 Fast Real-Time PCR System (Applied Biosystems) with SYBR Premix Ex Taq II (Tli RNaseH Plus) ROX plus (Takara Bio), with primers previously described in Yang et al. (2014). Two biological replicates, each one including three technical qPCR replicates, were performed. Results are given as the percentage of input normalized to Histone H2B.

ChIP-seq data analysis

Read mapping to the TAIR10 reference genome was performed using Bowtie 2 (Langmead & Salzberg, 2012). Intersection of peaks called in independent biological replicates confirmed the consistency between both replicates, which allowed us to pool them. Peak calling and differential enrichment analysis were carried out with the software SICER (Zang et al., 2009), using input as the control library with a redundancy threshold of 1, a window size of 200 bp, a gap size of 600 bp, and FDR = 0.01. The heatmaps and metagene plots were generated with SeqPlots (Stempor & Ahringer, 2016) using the normalized coverage files generated by SICER 2. Annotation of peak location relative to different genomic features was performed using PAVIS (Huang et al., 2013) with default parameters.

For the meta-analysis of gene expression levels and H2A.Z enrichment, genes were split into 6 groups based on TPM in WT Col-0 seedlings (TPMM<1,

TPM=1-5, TPM=5-10, TPM=10-30, TPM = 30-150, TPM>150), and mean H2A.Z enrichment was represented for each group with SeqPlots (Stempor & Ahringer, 2016). TF2Network tool (Kulkarni et al., 2018) was used to find over-represented transcription factors binding sites, and this information together with expression levels and H2A.Z enrichment levels were used to build a hierarchical network using cytoscape software (Shannon et al., 2003).

Supplementary data

All supplementary data files can be found at

http://plasticity.ibmcp.csic.es/downloads.html

Supplementary data 1: PFD physical interactions. Physical interactions retrieved from BioGrid, IntAct and MINT for all PFD subunits in *S. cerevisiae, D. melanogaster* and *H. sapiens.*

Supplementary data 2: Enriched GO terms in *S. cerevisiae* physical interactors.

Supplementary data 3: Genes coexpressed with PFD subunits. Genes coexpressed with PFD subunits in *S. cerevisiae* and *D. melanogaster,* with a Pearson correlation coefficient >0.6.

Supplementary data 4: Orthologs. Orthologs in *D. melanogaster* and *H. sapiens* of *Saccharomyces cerevisiae* PFD physical interactors.

Supplementary data 5: PFD interactors predicted in *Arabidopsis thaliana.*

Supplementary data 6: Differentially expressed genes. Differentially expressed genes found in *arp6, swc6* and *pfd3,5* mutants obtained with EdgeR, and table showing TPM normalized counts in every genotype and replicate.

Supplementary data 7: GO terms enriched among genes differentially expressed in *swc6, arp6* and *pfd3,5* mutants.

Supplementary data 8: Detected H2A.Z peaks in WT and *swc6* and *pfd3,5* mutants.

Supplementary data 9: Loci with differential H2A.Z levels in *swc6* and *pfd3,5* mutants.

Supplementary data 10: Coexpression and TF-DNA interaction network of genes downregulated in pfd3,5 mutant. The file contains all relevant data regarding nodes and edges' attributes for the use with Cytoscape, as depicted in Figure 25.

RESULTS

The canonical prefoldin complex is a heterohexamer present in all archaea and eukaryotes, formed by six different subunits named PFD1 to 6. It works in the cytoplasm as a co-chaperone associated with class II chaperones. In addition to the canonical subunits, eukaryote genomes have other genes encoding proteins with prefoldin tertiary structure, that together with PFD2 and PFD6 form an alternative complex with specialized functions called PFD-like (Chávez & Puerto-Camacho, 2016). Most nuclear roles discovered for prefoldin are described for subunits of the PFD-like complex, although some publications show evidence of a nuclear role for subunits of the canonical complex in yeast and metazoans. Considering this evidence and the high degree of conservation of PFD (Martín-Benito et al., 2002), we hypothesized that the canonical PFDc, or its individual subunits, would have a global role in the regulation of nuclear processes that is conserved in plants.

Cross-kingdom conservation of interactions between PFD subunits and nuclear proteins

The biological functions of a protein are largely determined by its interactions with other proteins. So, the first approach to test our hypothesis was to perform a data-mining analysis of reported physical interactors of the six PFD canonical subunits, comparing four phylogenetically distant organisms: *Saccharomyces cerevisiae, Drosophila melanogaster, Homo sapiens* and *Arabidopsis thaliana.*

Saccharomyces cerevisiae canonical PFD subunits have 870 known interactors (Supplementary file 1). Among them, 446 (51.3%) are nuclear, and 71 are common to 2 or more subunits (Figure 7A). We found numerous proteins involved in splicing, transcription, DNA replication, recombination and repair, and chromatin remodelling. An ontology analysis (Supplementary file 2) revealed a significant enrichment of cytoskeleton components, as expected, but also in chromatin components. Interestingly, the ontology "INO80-type complex" is significantly enriched with 14 proteins, with at least 7 of them being part of the Swr1 complex (Figure 7A).

To bolster the idea that these interactions could indicate a functional relationship between PFDs and certain nuclear processes, we examined the

genetic interactions described in yeast for the 6 PFD subunits and ranked the results (Figure 7B).

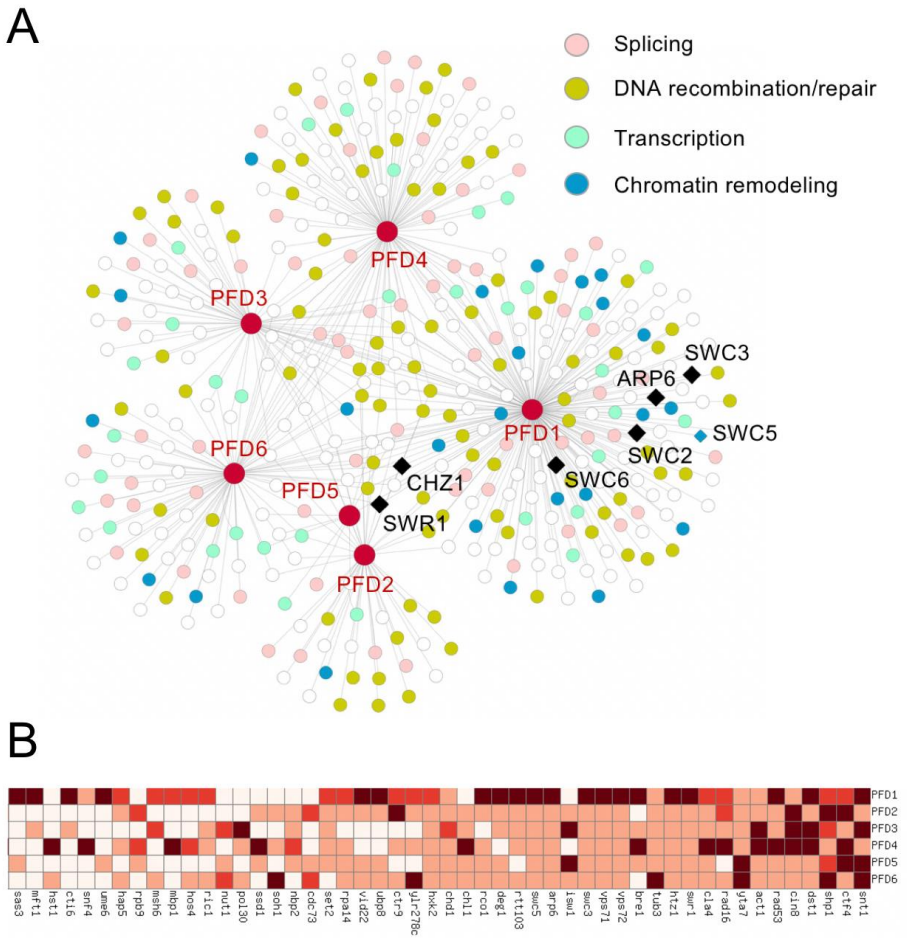

Figure 7. Physical and genetic interactions of yeast PFD subunits. (A) Network representation of physical interactions between PFD subunits and nuclear proteins, highlighting the functions related to DNA biology and subunits of the SWR1 complex. (B) Heatmap representing the top 50 stronger interactions with *PFD* genes. Genes with at least 1 physical interaction and 1 genetic interaction are shown. The darker the colour, the more evidence of interaction (see Methods).

Indeed, many of the physical interactions with nuclear proteins were further supported by genetic interactions not only with the interacting PFD subunit, but also with the other ones, suggesting that the nuclear function of the PFDs

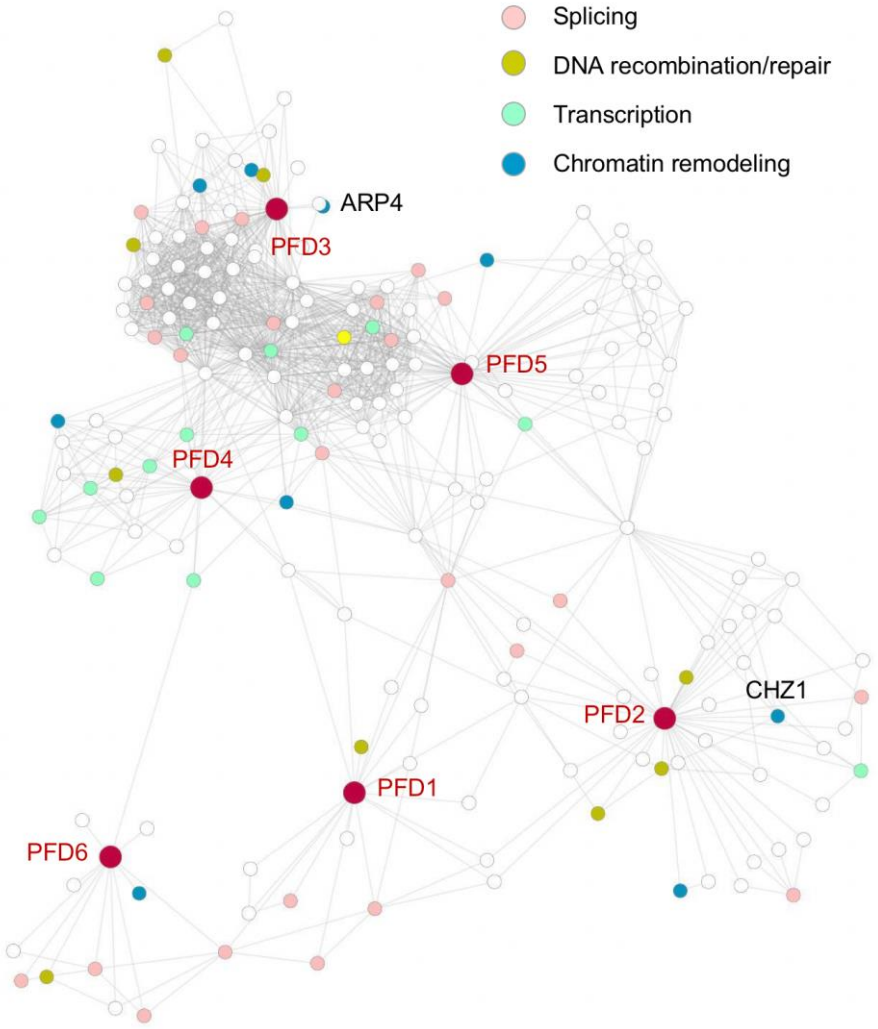

Figure 8. Network representation of the genes significantly coexpressed with *PFD* genes in yeast. Data were extracted from the YeastNet (v3) database, and the network was constructed using Cytoscape. CHZ1 and ARP4 are part of the yeast SWR1c.

is probably shared by the entire complex rather than any independent subunit. Again, the interaction with the Swr1 complex was significantly enriched, based on the presence of most Swr1 subunits at the top of the rank.

In addition, we searched for the genes that showed statistically significant co-expression with PFD genes in yeast, and found that 59.5% of them encoded nuclear-localized proteins, with functions related to chromatin remodelling, transcriptional regulation, splicing or DNA recombination and repair (Figure 8, Supplementary file 3).

These physical and genetic interactions and the significant co-expression values suggest that, at least in yeast, PFD might possess nuclear functions, notably in connection with chromatin remodelling, DNA repair, and splicing.

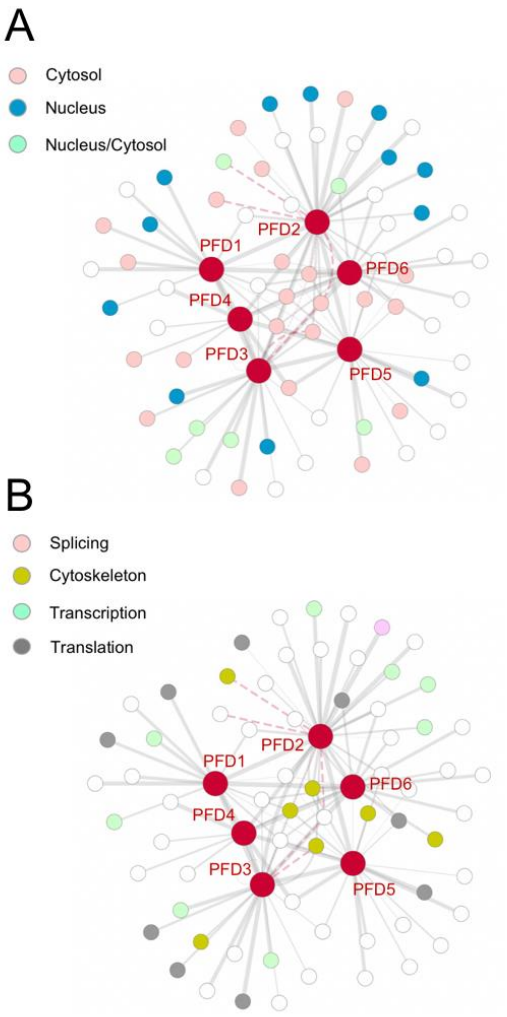

Figure 9. Network representation of physical and genetic interactors of PFD subunits in *D. melanogaster*. Genetic interactions are represented by dashed lines. The width of the edges is directly proportional to the coexpression value. (A) Subcellular localization of the interactors. (B) Functional categories of the interactors.

We obtained similar results analysing fly (Figure 9) and human PFD interactors (Supplementary file 1): a large group of cytosolic and cytoskeleton proteins and many nuclear interactors involved in splicing, transcription, chromatin and DNA metabolic processes.

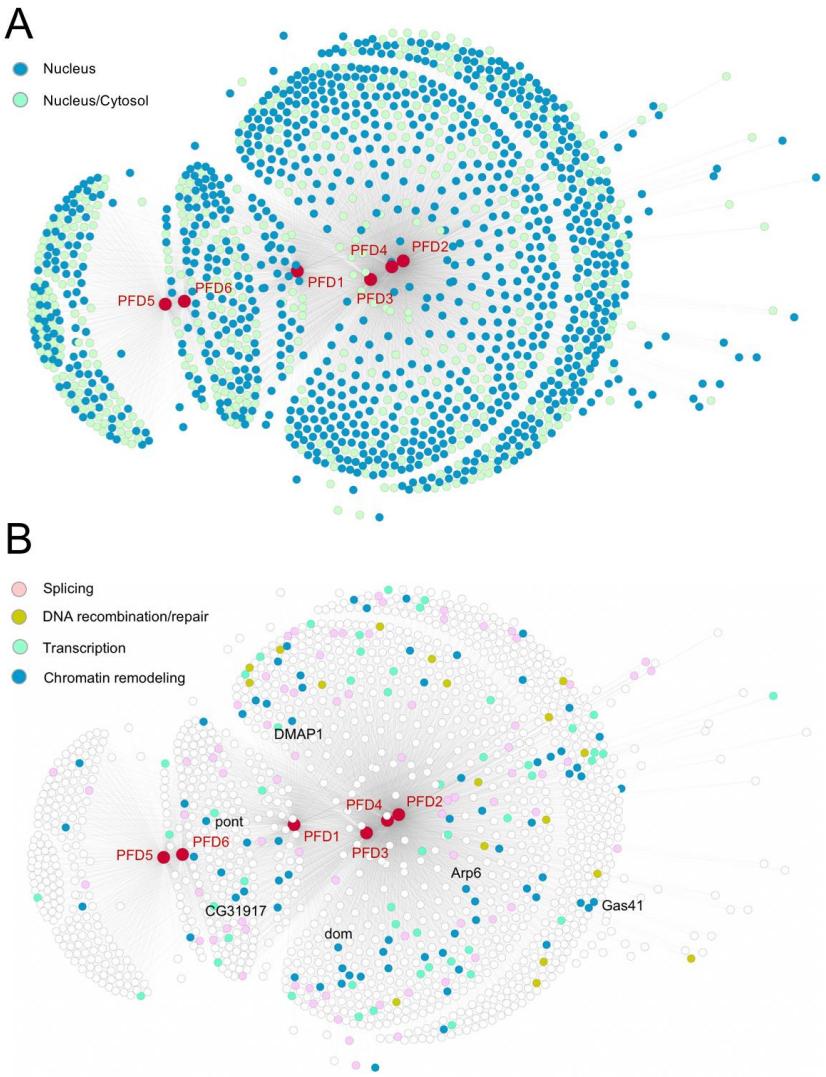

Figure 10. Network representation of the genes significantly coexpressed with *PFD* genes in *D. melanogaster*. Genes encoding subunits of the SWR1 complex are highlighted. (A) Subcellular localization of the interactors. (B) Functional categories of the interactors.

Interestingly, the functions represented by the human and fly interactors were strikingly conserved, although the identity of the particular interactors was different in most cases (only 17 of the 76 fly interactors, and 78 of the 445 human interactors, are orthologs of yeast interactors; see Supplementary file 4). As in the case of yeast, we found two members of the SWR1 complex among the human interactors, but none in *Drosophila.* Available data cover a low percentage of the proteome, specially in *Drosophila,* which may explain these results.

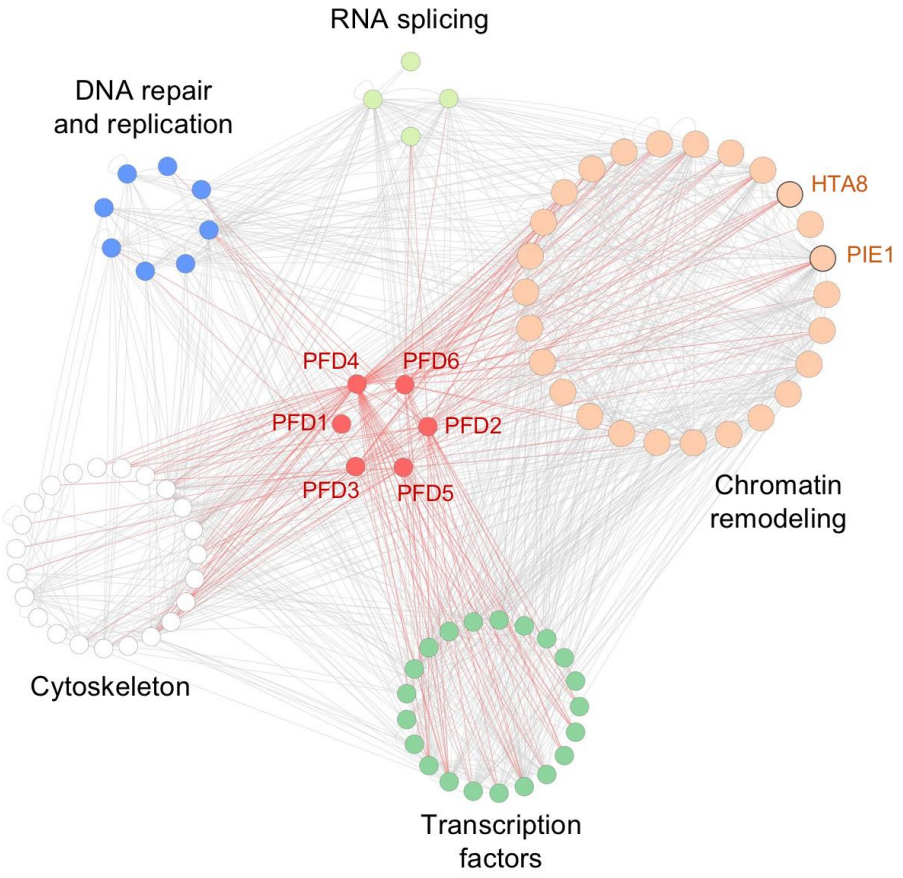

Figure 11. The predicted nuclear interactome of PFD in Arabidopsis. Physical interactions and co-expression values were obtained from the Arabidopsis Interaction Viewer (Geisler-Lee et al., 2007). Red edges represent statistically significant co-expression of genes with nuclear localization and PFD subunits.

Despite the lack of demonstrated physical interaction between PFD and SWR1c subunits in Drosophila, we did find significant co-expression between *PFD* genes and the *SWR1c* genes (Figure 10; Supplementary file 3), suggesting that the conservation of functional interaction between these two complexes might not be reduced to fungi, but would extend to metazoans.

The limited protein-protein interaction (PPI) data available for *Arabidopsis* in the BioGRID database shows only 8 PFD interactors. Considering the results obtained for yeast, fly and human, we decided to use the predicted interactome released by Geisler-Lee et al. (2007), based on interacting orthologs in several species, to gain some insight into the putative conserved roles that PFD could be performing in the nucleus. We used the *Arabidopsis Interactions Viewer* (Geisler-Lee et al., 2007) to obtain a network combining the predicted interactome, known PPIs and gene co-expression (Supplementary file 5).

As in the case of fungi and animals, the identity of the potential nuclear interactors for the *Arabidopsis* PFD subunits included transcriptional regulators and components of the DNA recombination and repair machinery, as well as proteins involved in RNA splicing (Figure 11). Noteworthy, 33% of interactors were involved in chromatin remodelling, such as subunits of the SWR1c, or SWI/SNF complexes (Supplementary file 5).

Given all the evidence for an extensive role of PFD in the nucleus, we set out to confirm the physical and functional connection between these proteins and at least one of the nuclear complexes identified in the *in silico* analysis. As stated in the introduction, the one characteristic that differentiates PFD in plants from that in other lineages is that its accumulation in the nucleus is dependent on DELLA protein levels (Locascio et al., 2013; Perea-Resa et al., 2017). For this reason, one of the criteria to select a nuclear complex for further investigation was the overlap between its known functions and those of DELLA proteins, such as the response to stress and the effect of flowering time. Several of the PFD potential interactors meet this criterium, such as the subunits of the chromatin remodelling SWR1 complex, and LSM proteins involved in RNA splicing and chromatin remodelling complexes. The interaction between PFD and LSM proteins has already been investigated (Esteve-Bruna et al., 2020), thus we decided to focus on the SWR1c, not only

for the seemingly overlap with DELLA functions, but also because it is specially represented, with numerous subunits present in our interaction data for fly, human, yeast, and the predicted *Arabidopsis* network.

PFD interacts physically with SWR1c in *Arabidopsis*

We performed a systematic and targeted yeast two-hybrid screening to test the interactions between *Arabidopsis* PFD and most of the SWR1c subunits (March-Díaz & Reyes, 2009). We found that each PFD subunit interacted with at least one of the components of SWR1c, but not with the three H2A.Z histones (Figure 12A).

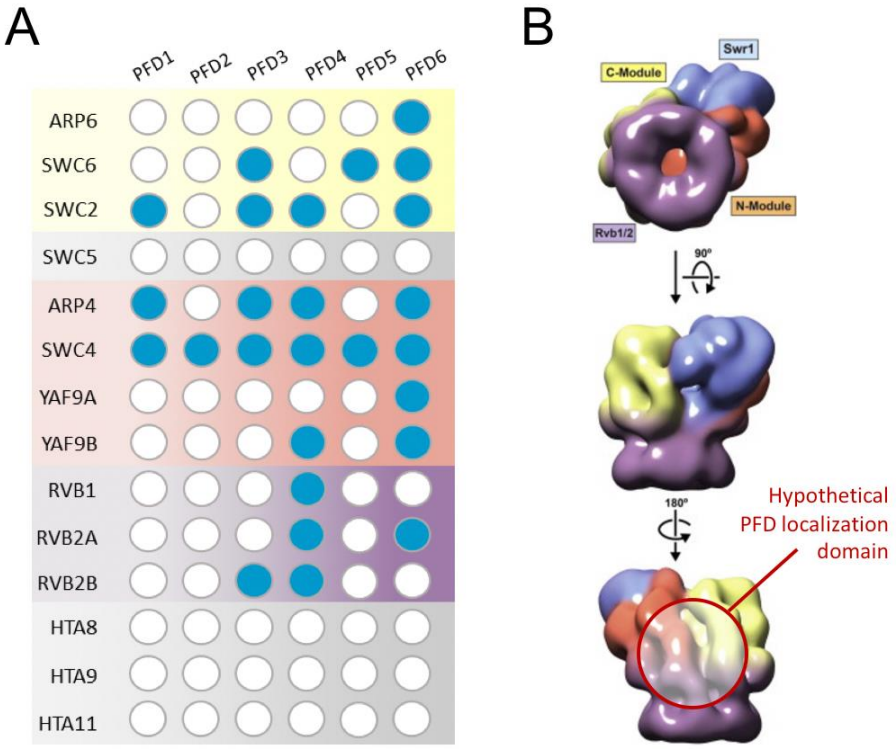

Figure 12. Physical interaction between PFD and the SWR1 complex. (A) Results of the yeast two-hybrid assays. Blue and white circles indicate interaction or no interaction, respectively. (B) Three-dimensional structure of the yeast SWR1 complex (adapted from Nguyen et al., 2013). Assuming that PFD would interact as a complex, the putative domain for the interaction is highlighted, based on the individual interactions detected.

This result is compatible with a model in which the interaction with SWR1c is established with the integral PFDc. Although the structure of the plant SWR1c has not been elucidated, it is possible to use the yeast structure as a likely model (Nguyen et al., 2013). Besides the SWR1 ATPase, three modules can be identified (The N-module, the C-module, and the RVB1/2 module). Considering the individual interactions detected by the yeast two-hybrid test, we hypothesize that the interaction surface with the PFDc would be mapped to the face opposite to the SWR1 ATPase with which the nucleosome interacts, based on the lack of interaction with the histones (Figure 12B).

Recently, affinity purification followed by mass spectrometry has also identified PFDs as ARP6- and SWC4-interacting proteins (Gómez-Zambrano et al., 2018; Luo et al., 2020; Potok et al., 2019; Sijacic et al., 2019). To obtain additional proof for the in vivo interaction between PFD and SWR1 subunits, we performed a co-immunoprecipitation assay between cMyc-ARP6 and YFP-PFD6 expressed in *N. benthamiana* leaves (Figure 13). As expected, we were able to detect cMyc-ARP6 after immunoprecipitation with anti-GFP only in leaves co-expressing both constructs.

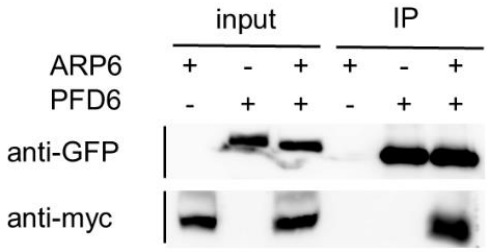

Figure 13. Interaction between cMyc-ARP6 and YFP-PFD6 detected by co-immunoprecipitation in agroinfiltrated *N. benthamiana* leaves.

Prefoldin contribute to the flowering time by affecting H2A.Z levels in the FLC

To explore if these interactions are physiologically relevant, we decided to investigate the flowering-time phenotype of *pfd* mutants, given that the

SWR1c has been involved in the regulation of this process (Lázaro et al., 2008; Martin-Trillo et al., 2006).

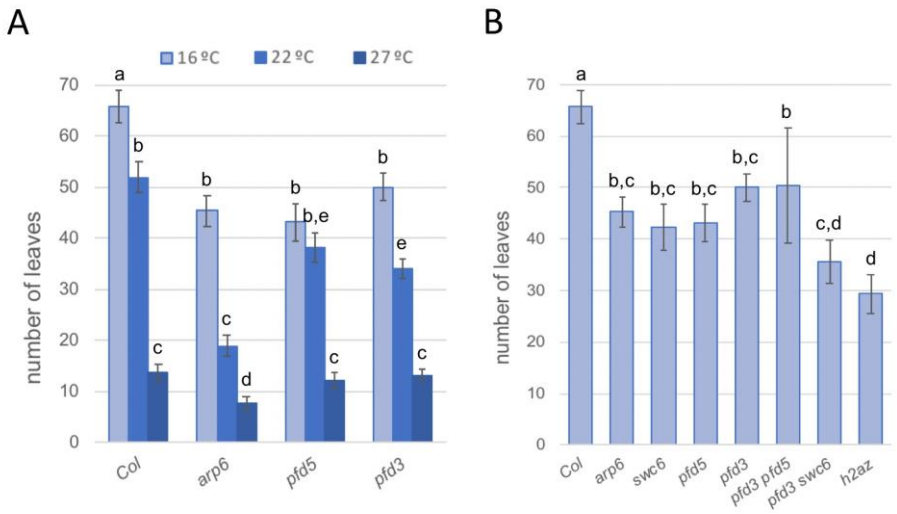

Figure 14. Flowering-time defects of *pfd* mutants. (A) Total number of leaves produced by wild-type, *arp6*, *pfd3* and *pfd5* mutants before flowering at three different growth temperatures under short days. (B) Total number of leaves of plants with *pfd* and *swr1c* mutant genotypes at 16ºC under short days. Small-caps letters indicate similar groups in an ANOVA test ($n \geq 12$, $p < 0.01$).

It has also been described that they act in the ambient temperature pathway for flowering (Galvão et al., 2015; Kumar et al., 2012; Kumar & Wigge, 2010), so we decided to analyse the flowering time of *arp6, pfd3* and *pfd5* mutants at 16, 22 and 27º C under short days (SD, Figure 14A), because the effect of the thermal induction of flowering is more marked in this condition. Consistent with previous reports, *arp6* flowered earlier than wild-type plants at all temperatures. At 22º and 16º C, *pfd* mutants showed early flowering, but at 27º C there was no significant difference with the wild type. The flowering-time defect of *pfd* mutants was less pronounced than that of *arp6* but showed the same tendency. At lower temperatures also *swc6* displayed early flowering, and there was only a marginal increase in this defect when combined with the *pfd3* mutation (Figure 14B), which would be in agreement with PFD and SWR1c mostly acting together, at least for the control of flowering time.

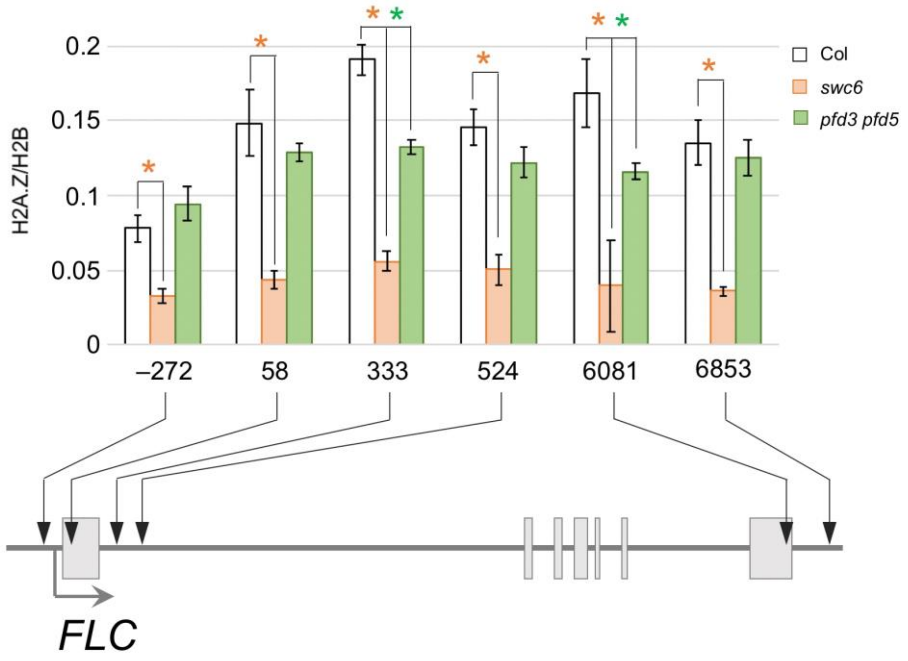

Figure 15. H2A.Z relative levels in the *FLC* locus. Plants were grown for 14 days at 22ºC in SD, before the onset of flower formation in the earlier-flowering genotype, and H2A.Z levels were determined by Chromatin immunoprecipitation (ChIP) coupled to qPCR using primers designed for the different regions of the FLC gene indicated by arrows. Numbers indicate the position, relative to the Transcription Start Site (TSS). Error bars indicate standard error (n=3). Asterisks mark statistically significant differences with respect to the wild-type values (Student's t-test, $p<0.05$).

The early flowering phenotype of mutants in the SWR1c can be explained by the reduced deposition of H2A.Z over the locus of the flowering repressor *FLC* that results in reduced expression (Deal et al., 2007). Given the early flowering phenotype of the *pfd* mutants and the physical interaction between PFD and SWR1c, we wondered whether this phenotype could be caused by reduced deposition of H2A.Z in the *FLC* locus as well. For that purpose, we analyzed the distribution of H2A.Z in the target locus by ChIP-qPCR in the WT and in the *pfd3,5* and *swc6* mutants grown for 14 days under SD conditions. Results in Figure 15 show that H2A.Z accumulates around the 5' and 3' ends of the gene in the WT, as described(Deal et al., 2007). The *swc6*

mutation strongly affects the accumulation of the histone variant, being reduced over the whole gene. This result is similar to the effects reported for mutants in other subunits (Deal et al., 2007; Gómez-Zambrano et al., 2018). Importantly, we also observed a reduction in H2A.Z deposition in the *pfd3,5* mutant, being the levels intermediate between the WT and the *swc6* mutant.

These results not only suggest that PFD activity may contribute to the control of flowering time through SWR1c, highlighting the physiological relevance of the interaction between both complexes but, more importantly, they indicate that PFDc may have positive role in SWR1c activity. Given these results, we decided to study the impact of the interaction at genomic level.

Transcriptomic analysis of PFDc and SWR1c loss-of-function mutants underscores overlapping functions

To obtain a more general picture of the effect of PFD upon SWR1c, we examined the genome-wide transcriptional defects of *pfd* mutants and compared it with those caused by loss of SWR1c activity. To this end, we performed RNA-seq analyses on the double *pfd3,*5 mutant and also on the *arp6* and *swc6* mutants, which harbour loss-of-function mutations in two different subunits of the SWR1c. The choice of *pfd3,5* is based on the assumption that PFD is acting as a complex, and that subunits 3 and 5 are essential for the formation of the complex (Martin-Benito et al., 2002). All plants were grown at 22º C in SD conditions, and samples were collected 2 weeks after germination to examine processes involved in vegetative growth.

Our analysis identified around 2700 misregulated genes (fold change [FC] ≥ 1.5; p value [*p*] ≤ 0.05; Supplementary file 6) in *arp6* and *swc6*, with half of them being up-regulated and half of them down-regulated. Moreover, a vast majority (70%) were misregulated in both mutants (Figure 16A), which is in agreement with current knowledge of the participation of both proteins in the activity of the SWR1c.

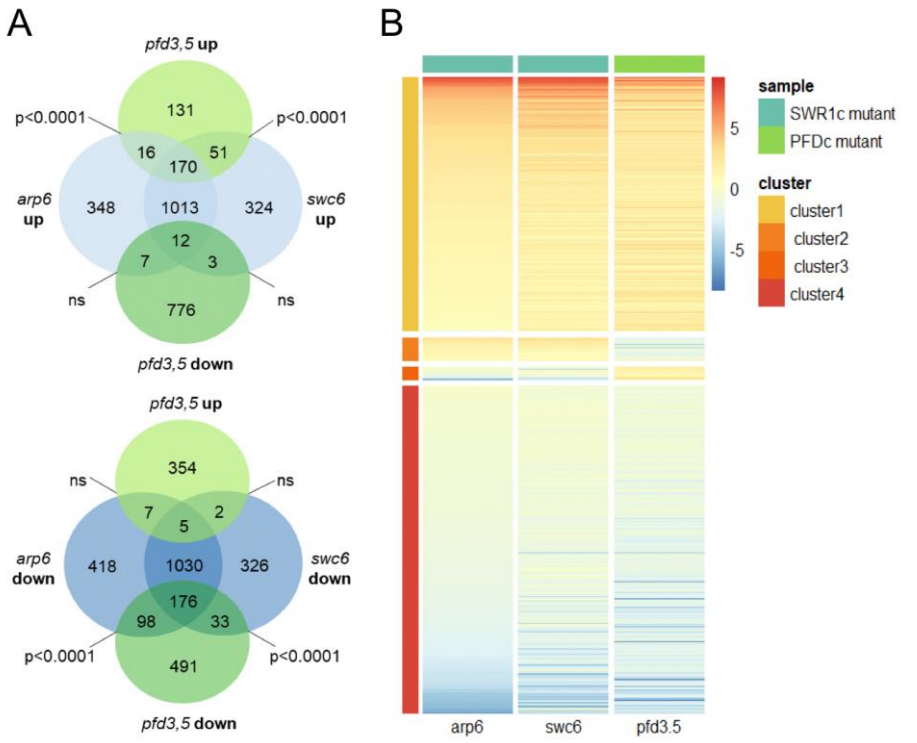

Figure 16. Transcriptomic changes in the double *pfd3,5* and the simple *swc6* and *arp6* mutants. (A) Venn diagrams showing the number of genes misregulated in each mutant (FC≥1.5, p≤0.05) and the overlap between them. Statistical significance of the overlap was calculated with a Fisher's exacts t-test. (B) Heatmap highlighting the large overlap in the sense of transcriptional changes in the PFDc and SWR1c loss-of-function mutants. Only the genes jointly misregulated in the three genotypes are shown.

An equivalent analysis of *pfd3,5* yielded 368 genes up-regulated and 798 genes down-regulated (Figure 16, Supplementary file 6). Importantly, 46.7% of the misregulated genes in *pfd3,5* overlap with the misregulated genes in *arp6* and *swc6* (Figure 16), Moreover, the transcriptional changes in the *pfd3,5* mutant follow the same tendency as the changes in the mutants affected in SWR1 activity: while 64.4% of the genes up-regulated in the *pfd3,5* mutant are common to up-regulated genes in the two SWR1c mutants, only 3.8% are common to the down-regulated genes (Figure 16); and similarly, 38.5% of the down-regulated genes in *pfd3,5* overlap with down-regulated genes in SWR1c mutants, while only 2.8% overlap with the set of up-regulated genes. This is

clearly showed in Figure 16B, where the fold change of every misregulated gene common to all mutants is represented in a colour scale, and genes are grouped according to their behaviour. Four clear clusters are formed: two large clusters where genes behave in the same way, up or down-regulated, and two small clusters where genes show opposite tendencies in "*swr1*" and "*pfd*" mutants.

Gene Ontology over-representation analysis among the genes misregulated in the two SWR1c mutants showed an enrichment in biological processes mostly related to defense response, response to stimulus and cell death, and also in categories like 'post-embryonic plant development' and 'mitotic cell cycle' (Figure 17; check Supplemental file 7 for a detailed list). These results are consistent with previous transcriptomic analyses with SWR1c mutant subunits (Berriri et al. (2016), Dai et al. (2017) and Sura et al. (2017)). Importantly, many of these functions were also enriched among the genes misregulated in the *pfd3,5* mutant, which included categories such as 'development cell growth and cell maturation', 'mitotic cell cycle', 'cell wall organization and biogenesis', 'photosynthesis', 'post-embryonic plant development and morphogenesis', and 'cell homeostasis', and also genes involved in subcategories included under 'response to stimulus' (Figure 17, Supplemental file 7).

Moreover, the categories over-represented in the set of genes regulated both by *arp6*, *swc6* and *pfd3,5* mutants are encased within general plant development, cellular processes and regulation: post-embryonic plant development and morphogenesis, root morphogenesis, lateral root development, trichoblast differentiation, plant epidermal cell differentiation, seed maturation and dormancy, phloem transport, cell wall modification, photosynthesis, mitotic cell cycle or cell homeostasis are some of the most enriched. On the other hand, there are also categories included in the response to stimulus and stress, like response to extracellular stimulus, response to starvation, response to water and water deprivation, response to insect, syncytium formation, response to toxic substances or glycosinolate metabolism. Moreover, there is an enrichment in genes involved in auxin and gibberellin biosynthesis and signalling pathway, two hormones that participate in the regulation of many of the processes mentioned above.

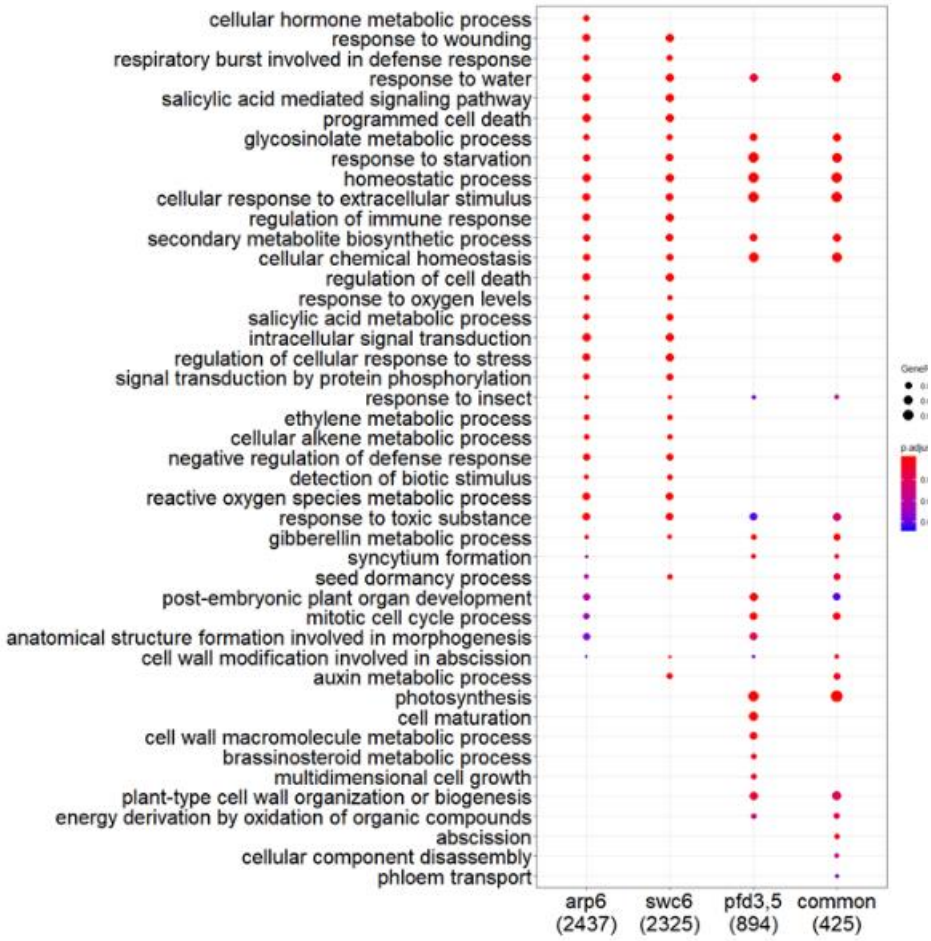

Figure 17. Gene Ontology enrichment analysis of misregulated genes in *arp6*, *swc6* and *pfd3,5* mutants. Numbers in brackets indicate the number of misregulated genes in each genotype.

The overlap in the gene targets and biological processes affected by mutants in the two complexes that indicate that the collaboration of PFDc with SWR1c function is rather extensive and not restricted to the regulation of the *FLC* locus (whose expression was not significantly misregulated in this experiment because of the developmental stage of the plants, long before the floral transition).

PFD affects H2A.Z deposition in a subset of genes

To further extend the study of the functional relationship between PFD and SWR1c, we analysed the genome-wide distribution of histone H2A.Z in WT and *pfd3,5* and *swc6* mutants by performing a ChIP-seq experiment on 14-day-old seedlings grown at 22º C in SD conditions. The two biological replicates were highly similar (supplemental figure 1), so we decided to pool them for further analysis.

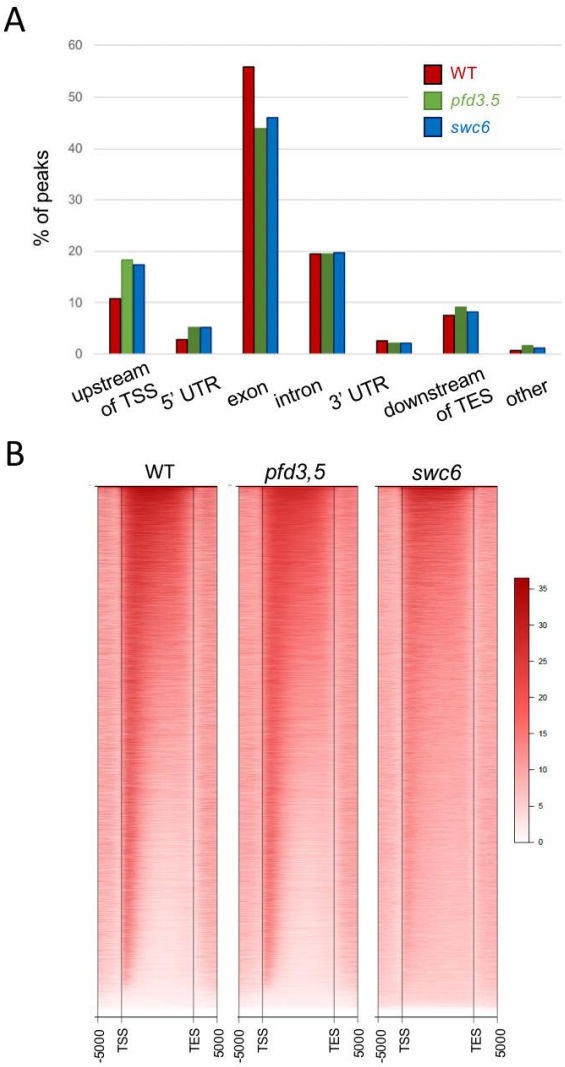

Figure 18. Genomic distribution of H2A.Z in wild-type, *pfd3,5* and *swc6* seedlings. (A) Distribution of H2A.Z in the different gene features. (B) Heatmap showing the genomic distribution of H2A.Z. TSS transcription start site, TES transcription stop site.

After peak calling, 18868 and 11414 peaks were detected in WT and *swc6* seedlings, respectively (Supplemental file 8), localised mainly in genic features (Figure 18A). According to previous publications (Coleman-Derr & Zilberman, 2012; Sura et al., 2017; Yelagandula et al., 2014), the accumulation profile in WT genotype shows strong enrichment of H2A.Z around the transcription start site (TSS), and smaller accumulation levels along the gene body and the 3' end (Figure 18B and 19A), while *swc6* mutant shows the same distribution but strongly decreased levels of the histone variant.

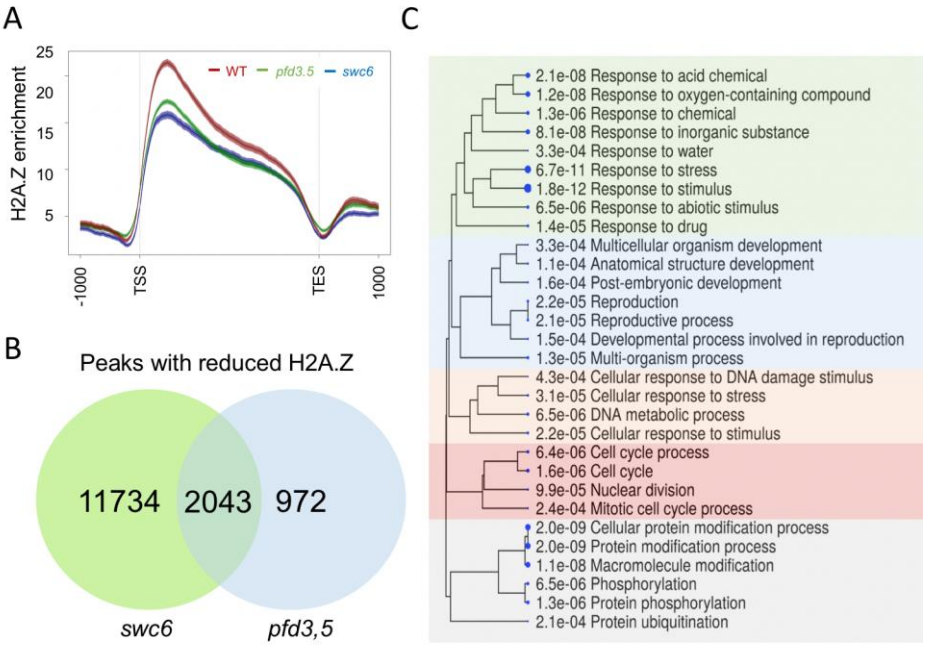

Figure 19. PFDs contribute to H2A.Z deposition in a subset of genes. (A) Metagene plot of H2A.Z enrichment in genes affected in *pfd3,5* mutant seedlings. (B) Venn diagram showing the overlap in peaks with reduced H2A.Z deposition. (C) Gene Ontology enrichment analysis of common genes affected by both mutations. TSS transcription start site, TES transcription stop site.

In *pfd3,5* seedlings, 19162 peaks were detected (Supplemental file 8), with slight reduction in the peak around the TSS in this mutant (Figure 18B). Indeed, a statistical analysis identified 3156 peaks with modest but significant decrease in H2A.Z enrichment (p adj. <0.01, Supplemental file 9). We also

detected 628 peaks with increased enrichment. The decreased peaks were annotated to 3015 different genes. A metagene plot representing only this subset of genes with reduced enrichment in the *pfd3,5* mutant clearly shows the reduction in the H2A.Z levels (Figure 19A).

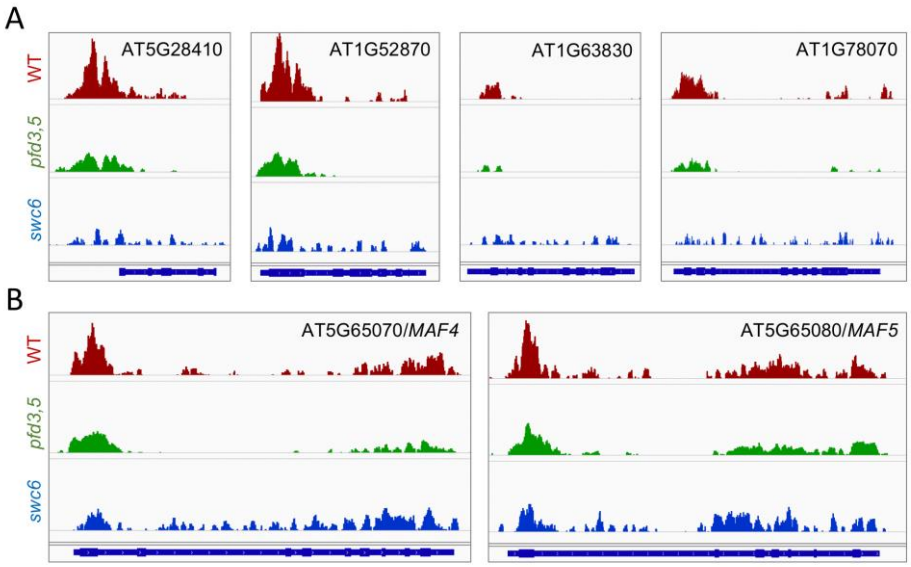

Figure 20. H2A.Z distribution in selected loci. (A) Top-rank genes with decreased H2A.Z levels in *pfd3,5* mutants. (B) *FLC* paralogs involved in flowering time control. Images were obtained with IGV. Exon/intron structures of the corresponding genes are shown at the bottom of each panel.

Importantly, 67.8% of the of the genes with decreased H2A.Z in *pfd3,5* (2043 genes) show decreased histone levels in *swc6* plants (Figure 19B and 20). It has been shown that the distribution of H2A.Z along one gene depends on its transcriptional behaviour (Figure 6). We wondered if PFDs affects H2A.Z deposition depending on the transcription level of the gene. For that purpose, we first grouped genes in sextiles of expression based on the expression level found in our RNA-seq analysis of WT seedlings, and then plotted the average H2A.Z levels for the WT, *pfd3,5* and *swc6* for each group (Figure 21). Results showed that H2A.Z deposition was affected in the *swc6* mutants regardless of the expression level of the gene, as expected for a mutant affecting a core

subunit of the SWR1c. Nonetheless, defects were more apparent in gene groups with lower expression levels in the *pfd3,5*. Note that the H2A.Z distribution in the gene group with the highest expression level in the *pfd3,5* mutant is indistinguishable of the WT. These results suggest that PFD's contribution to H2A.Z deposition is more relevant in genes with lower expression level, likely associated to gene responsiveness. This is in agreement with the GO analysis (Figure 19C), that showed that several categories associated to responses to the environment were enriched among the common genes affected in *swc6* and *pfd3,5* mutants.

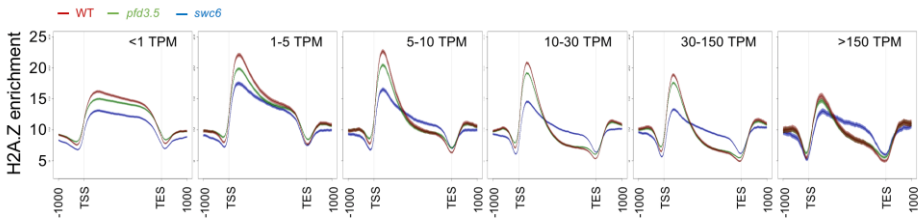

Figure 21. Metagene plots showing H2A.Z levels over different subsets of genes grouped according to their expression levels (indicated in TPM (transcripts per million mapped reads). TSS transcription start site, TES transcription stop site.

Network analysis identifies candidate TFs acting downstream of PFD-SWR1c

In agreement with previous observations (Gómez-Zambrano et al., 2018) in which most genes downregulated in *swr1c* mutants did not suffer from defects in H2A.Z deposition, we did not find a large overlap between the sets of misregulated genes and those with reduced H2A.Z in *pfd3,5* (Figure 22). Although this overlap was statistically significant, only 4% of the genes with defective H2A.Z deposition were downregulated in the case of *pfd3,5*, and 5% in the case of *swc6* (Figure 22).

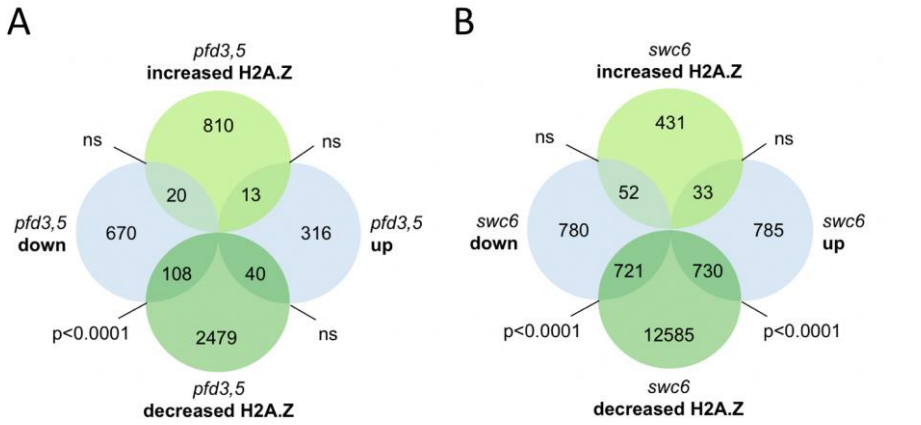

Figure 22. Overlap between H2A.Z and expression defects in *pfd3,5* (A) and *swc6* (B) mutants.

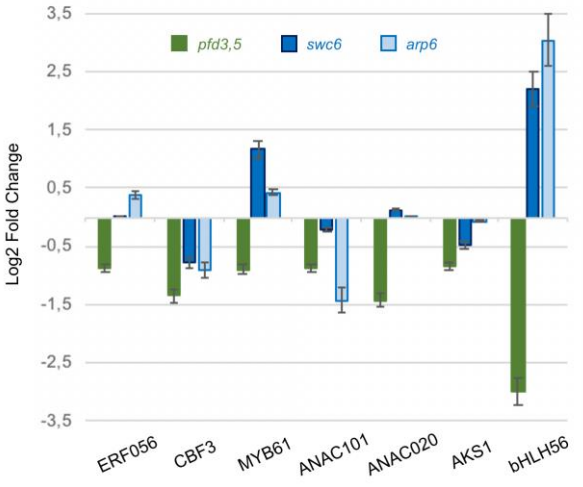

Figure 23. Expression levels of selected TFs with defective H2A.Z deposition. The Log2 Fold Change values were extracted from the RNA-seq experiments described above (Figure 16).

Thus, it is likely that most of the genes misregulated in *pfd3,5* are indeed targets of only a handful of TFs whose expression is regulated by H2A.Z deposition. To investigate this possibility and identify the primary targets for PFD-dependent SWR1c activity, we extracted the list of TFs present among the 798 downregulated genes in *pfd3,5* which had also been tagged for defective H2A.Z levels. We found only 7 matching these criteria (Figures 23 and 24).

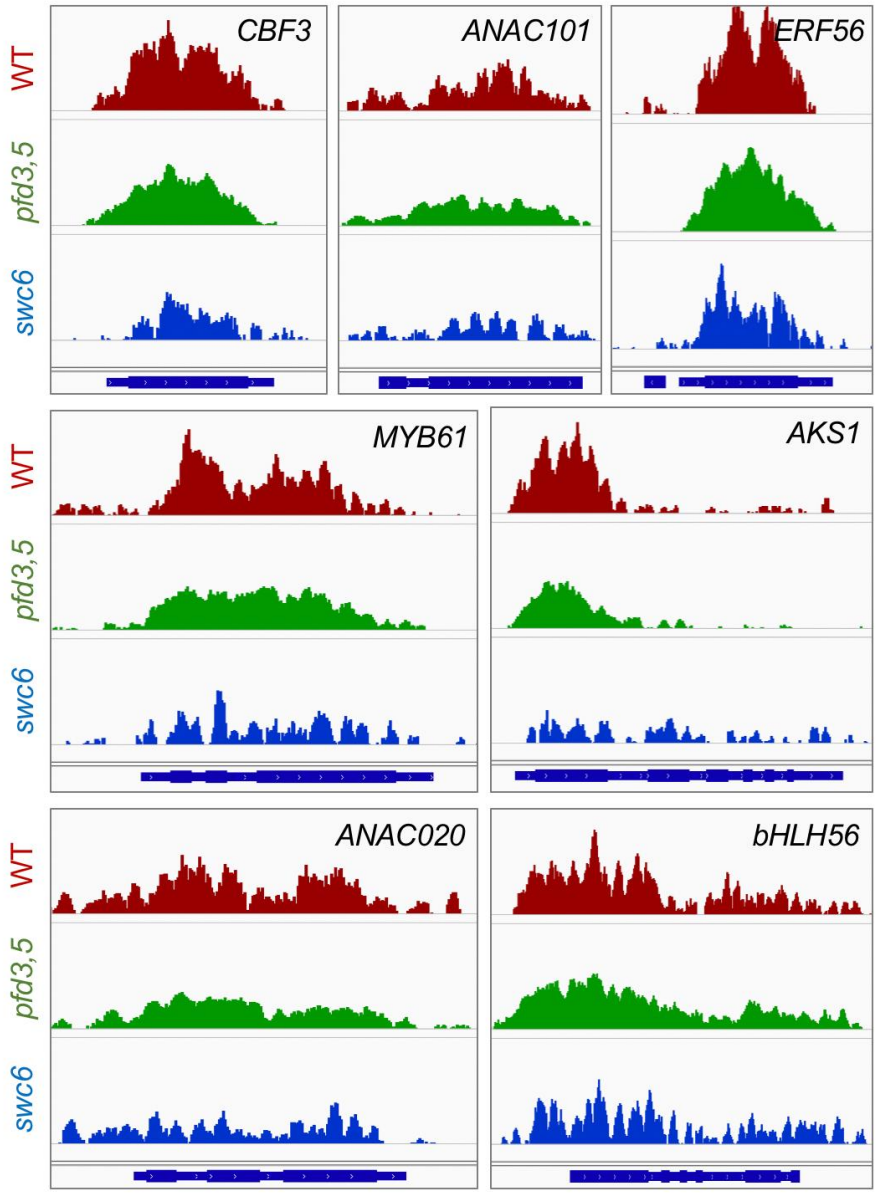

Figure 24. H2A.Z distribution in the 7 selected TFs that display lower expression levels in the *pfd3,5* mutant. Images were obtained with IGV. Exon/intron structures of the corresponding genes are shown at the bottom of each panel.

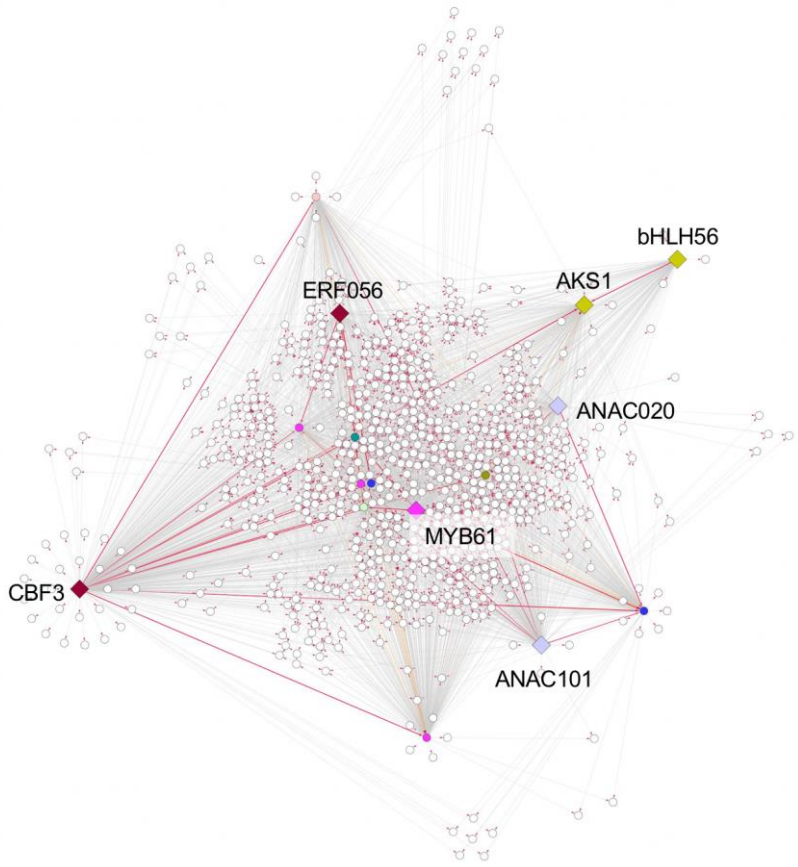

Figure 25. Hierarchical interaction analysis of the co-regulation of the genes downregulated in *pfd3,5* mutants by TFs affected in H2A.Z deposition in the same mutant. Coloured nodes indicate TFs in the set of downregulated genes which are predicted to regulate other genes in the same set. Diamonds mark those TFs that also show defects in H2A.Z deposition in the *pfd3,5* mutant. Red edges highlight transcriptional regulation between TFs. Red arrowheads indicate the direction of the regulation. Hierarchical interactions were calculated and represented with Cytoscape.

To find the possible connections between these 7 TFs and the rest of the genes downregulated in *pfd3,5*, we used the TF2Network tool (Kulkarni et al., 2018). This algorithm identifies putative regulatory relationships based on experimental genome-wide evidence of TF binding to promoters, and co-expression values. With those criteria, we found that the first tier of 7 TFs were predicted to regulate 752 out of the 798 downregulated genes ($p<0.01$

as confidence threshold value) (Figure 25). Moreover, this set of 752 genes formed a very robust network because the algorithm also highlighted the enrichment of a second tier of 8 additional TFs whose H2A.Z levels were not significantly affected in the pfd3,5 mutant, but their expression levels were lower and were direct targets of the first-tier TFs (Figure 25, Supplemental file 10).

These results provide an explanation for the large number of genes whose expression is regulated by PFD but do not seem to have H2A.Z defects in *pfd* loss-of-function mutants. However, they do not explain two observations: why many of the genes with altered H2A.Z deposition in *pfd* or *swr1c* do not have defects in expression levels, and why only a small subset of loci regulated by SWR1c are also regulated by PFD. To clarify this second issue, we decided to investigate the possible molecular mechanisms by which PFD could affect SWR1c activity.

Possible molecular mechanisms of PFD effect on SWR1c

Given the physical interaction found between PFD6 and ARP6, and the role of PFD as a co-chaperone, we considered that a plausible model is that PFD is directly altering SWR1c activity by affecting ARP6 protein levels. As reference, we used the abundant, unrelated protein DET3. Figure 26A shows the results of the Western analysis. We found lower levels of ARP6 in the *swc6* mutant compared to the WT. This result suggests that loss of one core subunit of the complex leads to lower accumulation of another, likely as consequence of decreased stability when the whole complex cannot be assembled. We are currently unable to determine whether this extends to other mutants and subunits of SWR1c, so it remains as an open question to be resolved in the future. Importantly, no apparent changes in the level of ARP6 was found in any *pfd* mutant background. This analysis indicates that impairment of PFD function has no impact on ARP6 protein levels. However, our yeast 2-hybrid results (and the *in silico* interactome studies) indicate that other subunits of SWR1c also interact with PFDc, so the possibility is still open that the levels of other subunits are affected in *pfd* mutant backgrounds.

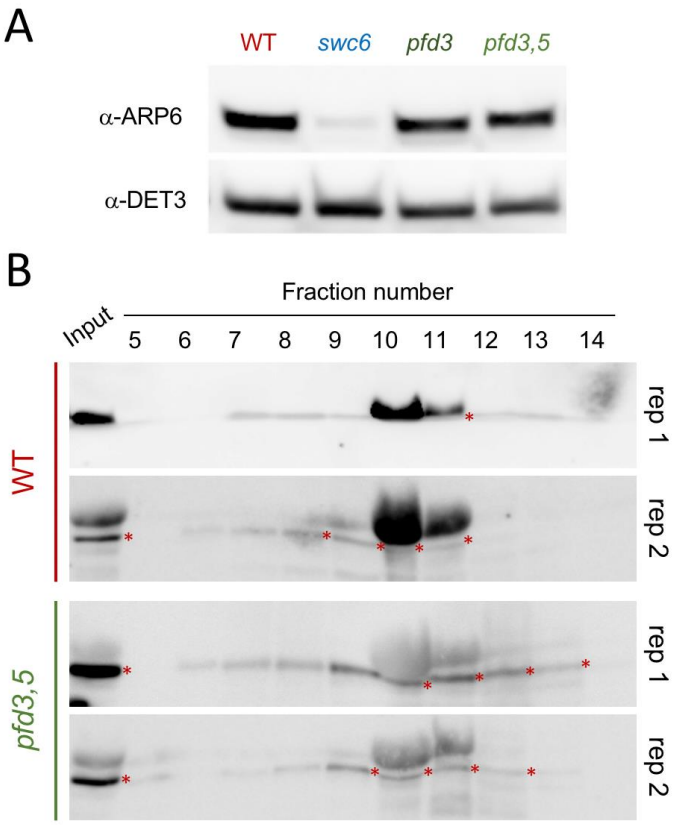

Figure 26. Analysis of the integrity of the SWR1c in *pfd3,5* mutants. (A) Western blot analysis of ARP6 protein levels in total extracts of seedlings with different genotypes. (B) Gel filtration and Western blot analysis of the levels and relative size of the SWR1c in WT and *pfd3,5* mutants. Two independent replicate experiments are shown. Fraction 9 ≈ 670kDa, fraction 11 ≈ 445 kDa, fraction 12 ≈ 150 kDa.

According to the role of PFD as co-chaperones of the chaperonin CCT, recent results indicate that the PFDc assistance to CCT is also required in the nucleus of human cells, in particular, for the assembly of the histone deacetylase HDAC1 into transcriptional repressor complexes (Banks et al., 2018). Thus, we next tested the possibility that PFD are required for the assembly or for keeping the integrity of SWR1c. To test this, we subjected extracts of WT and *pfd3,5* seedings to size exclusion chromatography. The rationale behind is that any alteration in the assembly or in the posterior

integrity will result in SWR1 complex versions of different size. We followed the elution profile of the complex by immunoblots, using an anti-ARP6 antibody. Figure 26B shows that the SWR1c eluted in fractions corresponding to the reported size of the complex (Deal et al., 2007). Notice that the band corresponding to ARP6 is marked with an asterisk. The elution profile was very similar in the *pfd3,5* mutant. This result indicates that the lack of at least PFD3 and PFD5 activities does not have any effect in the assembly or integrity of the SWR1c.

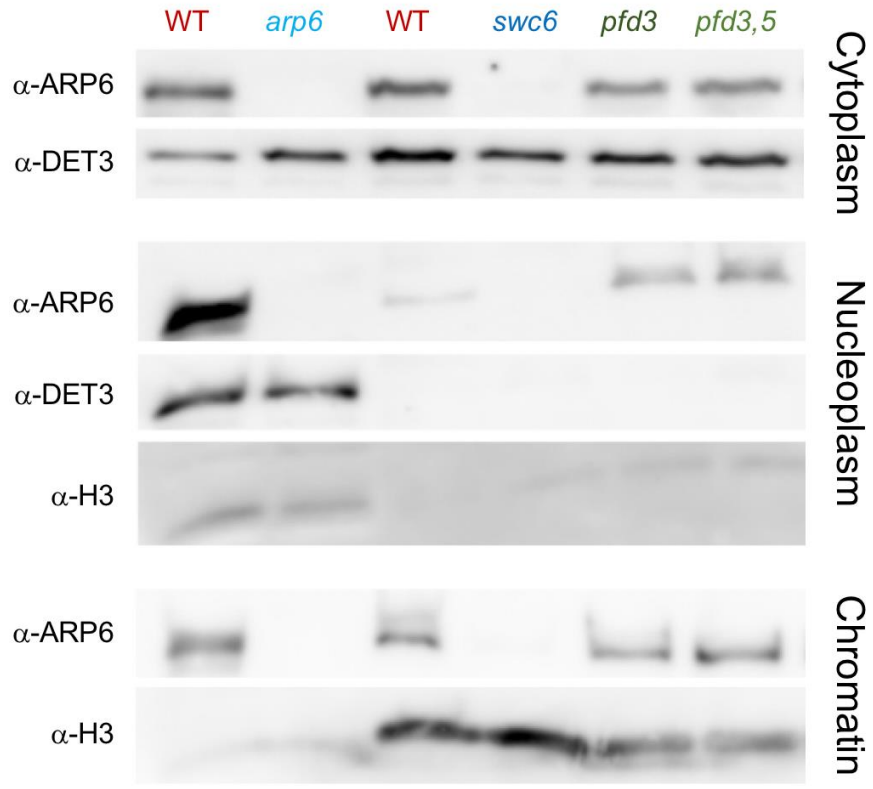

Figure 27. Cell fractioning shows overaccumulation of the ARP6 subunit in the nucleoplasm of *pfd* mutants. Proteins from the different cellular fractions were subjected to Western analysis. H3 and DET3 proteins were used as controls for chromatin and cytoplasm fractions, respectively. First two lanes correspond to WT and *arp6* total protein extracts loaded as control for all proteins detected.

The above results led us to test whether it is the activity of SWR1c, rather that its levels or integrity, what is affected by PFDs. Given that SWR1c activity takes place in the chromatin, we investigated if PFD affected the recruitment of the SWR1c to this particular location. For that purpose, we did a cellular fractionation of extracts of seedlings of *pfd* single and double mutants. We followed the presence of the complex in each fraction by immunoblots with anti-ARP6 antibodies. As controls we used extracts of the seedlings carrying the *swc6* mutation, in which the ARP6 levels are reduced. We found the ARP6 protein in all fractions (Figure 27). This result was surprising to us, as we expected it to be preferably at the chromatin (see for instance the H3 marker found only in chromatin fractions). Nonetheless, its presence in the cytoplasm may suggest that the complex is assembled in this location, prior to its import into the nucleus, a hypothesis that would be very interesting to pursue in the future. Interestingly, we found a seemingly higher proportion of ARP6 in the nucleoplasm in the *pfd3* and *pfd3,5* mutants compared with the WT, although no apparent differences were observed in the chromatin. At present, we are not sure about the relevance of this result. The accumulation of ARP6 in the nucleoplasm of the mutants may have a small, yet not noticeable by western analysis, effect in the pool of chromatin-bound SWR1c, affecting only H2A.Z deposition in loci highly sensitive to SWR1c levels. This possibility fits with the ChIPseq data, which indicate that the PFD effect on H2A.Z deposition is restricted to a subset of genes.

DISCUSSION

This Thesis was motivated by previous observations suggesting that PFD was in the nucleus of plant cells not only as a mechanism for regulation of its cytosolic function as a co-chaperone, but also to perform additional roles in this compartment. Those observations included the physical interaction of one specific subunit of human PFD with a TF (Hagio et al., 2006; Mori et al., 1998; Satou et al., 2001; Watanabe et al., 2002), and the misregulation of gene expression in yeast *pfd* mutants (Millán-Zambrano et al., 2013). The work presented here has expanded our knowledge about the possible role of PFD in the nucleus in two directions: (i) it has established the large dimension of the nuclear interactome of PFD in fungi, animals and plants; and (ii) it has demonstrated the functional relevance in chromatin remodelling of the interaction between the Arabidopsis PFD and the SWR1 complex.

In depth analysis of publicly available protein-protein databases for several organisms like *S. cerevisiae*, *D. melanogaster* and *H. sapiens* has conveyed the view of PFD as a hub in the cellular interaction networks. The robustness of this analysis relies on the fact that all these datasets have been generated by experimental data, and it is supported by additional evidence, such as the statistically significant co-expression between PFD subunits and their interacting partners. The same holds true for the predicted interactome of the Arabidopsis PFD, and the most striking observation is the strong conservation of PFD's nuclear interactome across kingdoms. Interestingly, the identity of the elements in this conserved interacting network draws the attention to multiple nuclear functions: apart from DNA replication and repair, PFD would not only regulate gene expression through the interaction with DNA-binding TFs, but also via the interaction with chromatin remodelling and RNA splicing complexes. In a parallel effort in our lab, new experimental evidence has been gathered to confirm the biological relevance of the interaction between PFD and the LSM2-8 complex –one of the main modules regulating RNA splicing (Esteve-Bruna et al. 2020). In that case, PFD has been found to serve LSM8 as a client protein to the Hsp90 chaperone, and thus regulate the levels of the active spliceosome. Accordingly, loss of PFD function has been shown to impact alternative splicing of multiple genes, particularly under cold-stress situations. In this Thesis, we have focused on the possible relevance of the interaction between PFD and the SWR1 complex to confirm the requirement of this co-

chaperone for the correct H2A.Z deposition in genes regulated through this mechanism.

The first question that arises from these studies is whether the interaction with the nuclear machinery (i) involves all PFD subunits, as a complex; (ii) reflects new activities of the individual PFD subunits; or (iii) occurs through the participation of PFD subunits in alternative complexes. There is experimental evidence that is compatible with all posibilities. On one hand, unpublished observations in the lab examining the phenotype of all single *pfd* mutants as well as higher-order mutants including the sextuple *6xpfd* mutant, indicate a very large functional overlap between all PFD subunits (Blanco-Touriñán et al, manuscript in preparation). This is further supported by the structural requirements of PFD subunits, for which only the already solved cytosolic jelly-fish structure is thermodinamically possible (Martín-Benito et al. 2002). Moreover, recent large-scale proteomic studies in a set of 13 plant species has shown two relevant characteristics: (a) the abundant level of the PFDc in plant cells allows easy by-the-eye detection of co-elution patterns for all subunits in all plants examined; and (b) the same co-elution pattern is obtained from nuclear and whole-cell extracts (McWhite et al., 2020).

On the other hand, alternative complexes involving only some PFD subunits, as well as PFD-like proteins, have also been found in animal cells (Chávez & Puerto-Camacho, 2016). Given that these PFD-like proteins have orthologs in plants, it is likely that some of the nuclear functions of PFD are achieved through these complexes.

The second relevant question is the mechanism by which PFD would be required for the correct function of SWR1c. At least four mechanisms could be envisioned:

1. The regulation of the level of one or more of the SWR1c subunits. This would be equivalent to the mechanism by which PFD regulates the function of the LSM2-8 complex (Esteve-Bruna et al., 2020), and is in tune with the known role of PFD as a co-chaperone. However, our analysis of the levels of the direct interacting subunit (ARP6) do not support a general reole for PFD in the regulation of the levels of active SWR1c, at least under optimal growth conditions. It might be possible that this would be different under, for instance, sub-optimal

temperatures –given the known role for SWR1c in these responses–, but this would not explain the large effect observed in H2A.Z deposition in *pfd3,5* mutants at an optimal growth temperature.

2. The regulation of the composition of the SWR1c. We examined this possibility through gel filtration assays, which allow the identification of changes in the size of the SWR1c. However, no shift in size was observed in the *pfd3,5* mutant in different attempts, suggesting that this mechanism is unlikely.
3. The regulation of the localization of SWR1c in the appropriate cell compartment. As a chromatin remodelling complex, active SWR1c can be found attached to chromatin in cell fractionation assays, and this localization was not significantly altered in *pfd3,5* mutants. However, our assay provides information at the whole genome scale, and it does not rule out the possibility that PFD is required for the access of SWR1c to the chromatin only in specific loci. Additional ChIP-qPCR experiments of tagged ARP6 or SWC6 in potential target loci will help establish the likelihood of this mechanism.
4. The regulation of the activity of SWR1c. It is possible that SWR1c does not require PFD to access the correct target loci, and that its levels are not dependent on the interaction with PFD, but that PFD is required for full histone-exchange activity of SWR1c. The observation that PFD interacts with peripheral subunits -rather than the core PIE1 subunit- reduces the likelihood of this mechanism, but it cannot be completely ruled out.

The third important question is what PFD may add to the regulation of SWR1c function: does PFD relay environmental information to the activity of this complex? Is it necessary to recognize a certain subset of target loci? Does it provide only homeostatic regulation to the levels/activity of SWR1c? There are no indications that the expression of PFD genes is influenced by the environment. However, the GO enrichement analysis of genes misregulated in *pfd3,5* mutants and, more importantly, of loci with defective H2A.Z levels, yields categories involved in the response to different environmental stimuli, which is in support of this possibility. Moreover, it is important to remark that, while PFD levels in the nucleus seem to be constant

in yeast and animal cells, the levels of nuclear PFD in Arabidopsis largely (but not fully) depend on the accumulation of DELLA proteins (Locascio et al., 2013; Perea-Resa et al., 2017). Given that DELLA protein accumulation is a proxy for environmental conditions, it is tempting to speculate that the functions of nuclear PFD –including the regulation of SWR1c-dependent H2A.Z deposition– are enhanced or inhibited to adjust cellular functions to the external environment. Preliminary observations examining genome-wide H2A.Z deposition in *dellaKO* mutants indicate that DELLA proteins indeed participate in establishing the appropriate H2A.Z landscape in thousands of loci, even more than PFD itself. This quantitative discrepancy might suggest that, apart from the regulation via PFD, DELLA proteins could regulate H2A.Z deposition either through direct interaction with SWR1c, through the interaction with the INO80 complex involved in H2A.Z removal, or through the interaction with other complexes that modulate, for instance, H2A.Z post-translational modifications. Further work in the lab will clarify these possibilities.

Finally, it is important to remark that the *in silico* comparative analysis of the nuclear PFD interactome points to yet unexplored connections with important functions in nuclear biology, such as DNA replication and DNA repair. Whether PFD acts as a wide-spectrum molecular co-chaperone in both the nucleus and the cytosol is an attractive hypothesis that would be worth pursuing. A similar view has been already proposed for human small Heat Shock Proteins that prevent the aggregation of multiple substrates (Mymrikov et al., 2017)

CONCLUSIONS

1. The presence of prefoldin in the nucleus and its interaction with nuclear machinery is conserved across kingdoms.

2. Among the multiple potential functions of prefoldin in the nucleus, the interaction with subunits of the SWR1 complex is biologically relevant, based on the defects in H2A.Z deposition observed in *prefoldin* mutants.

3. The significant overlap between prefoldin and SWR1c target genes indicates that both complexes coregulate functions related to environmental responses.

4. The specific mechanism by which prefoldin affects SWR1c activity is still unknown, but several observations suggest that SWR1c requires prefoldin to deposit H2A.Z in only a subset of the target loci, instead of being a general requirement.

REFERENCES

Abe, A., Takahashi-Niki, K., Takekoshi, Y., Shimizu, T., Kitaura, H., Maita, H., Iguchi-Ariga, S. M. M., & Ariga, H. (2013). Prefoldin plays a role as a clearance factor in preventing proteasome inhibitor-induced protein aggregation. *Journal of Biological Chemistry*. https://doi.org/10.1074/jbc.M113.476358

Altaf, M., Auger, A., Monnet-Saksouk, J., Brodeur, J., Piquet, S., Cramet, M., Bouchard, N., Lacoste, N., Utley, R. T., Gaudreau, L., & Côté, J. (2010). NuA4-dependent acetylation of nucleosomal histones H4 and H2A directly stimulates incorporation of H2A.Z by the SWR1 complex. *Journal of Biological Chemistry*, *285*(21), 15966–15977. https://doi.org/10.1074/jbc.M110.117069

Anders, S., Pyl, P. T., & Huber, W. (2015). HTSeq-A Python framework to work with high-throughput sequencing data. *Bioinformatics*, *31*(2), 166–169. https://doi.org/10.1093/bioinformatics/btu638

Arana, M. V., Marín-De La Rosa, N., Maloof, J. N., Blázqueza, M. A., & Alabadí, D. (2011). Circadian oscillation of gibberellin signaling in Arabidopsis. *Proceedings of the National Academy of Sciences of the United States of America*, *108*(22), 9292–9297. https://doi.org/10.1073/pnas.1101050108

Banks, C. A. S., Miah, S., Adams, M. K., Eubanks, C. G., Thornton, J. L., Florens, L., & Washburn, M. P. (2018). Differential HDAC1/2 network analysis reveals a role for prefoldin/CCT in HDAC1/2 complex assembly. *Scientific Reports*. https://doi.org/10.1038/s41598-018-32009-w

Barski, A., Cuddapah, S., Cui, K., Roh, T. Y., Schones, D. E., Wang, Z., Wei, G., Chepelev, I., & Zhao, K. (2007). High-Resolution Profiling of Histone Methylations in the Human Genome. *Cell*, *129*(4), 823–837. https://doi.org/10.1016/j.cell.2007.05.009

Berriri, S., Gangappa, S. N., & Kumar, S. V. (2016). SWR1 Chromatin-Remodeling Complex Subunits and H2A.Z Have Non-overlapping Functions in Immunity and Gene Regulation in Arabidopsis. *Molecular Plant*, *9*(7), 1051–1065. https://doi.org/10.1016/j.molp.2016.04.003

Billon, P., & Côté, J. (2012). Precise deposition of histone H2A.Z in chromatin for genome expression and maintenance. In *Biochimica et Biophysica Acta - Gene Regulatory Mechanisms* (Vol. 1819, Issues 3–4, pp. 290–302). https://doi.org/10.1016/j.bbagrm.2011.10.004

Biterge, B., & Schneider, R. (2014). Histone variants: Key players of chromatin. *Cell and Tissue Research*, *356*(3), 457–466. https://doi.org/10.1007/s00441-014-1862-4

Bogumil, D., Alvarez-Ponce, D., Landan, G., McInerney, J. O., & Dagan, T. (2013). Integration of Two Ancestral Chaperone Systems into One: The Evolution of Eukaryotic Molecular Chaperones in Light of Eukaryogenesis. *Molecular Biology and Evolution*, *31*(2), 410–418. https://doi.org/10.1093/molbev/mst212

Cao, S., Carlesso, G., Osipovich, A. B., Llanes, J., Lin, Q., Hoek, K. L., Khan, W. N., & Ruley, H. E. (2008). Subunit 1 of the Prefoldin Chaperone Complex Is Required for Lymphocyte Development and Function. *The Journal of Immunology*. https://doi.org/10.4049/jimmunol.181.1.476

Chávez, S., & Puerto-Camacho, P. (2016). Prefoldins. In *eLS* (pp. 1–8). John Wiley & Sons, Ltd. https://doi.org/10.1002/9780470015902.a0026334

Choi, K., Kim, S., Kim, S. Y., Kim, M., Hyun, Y., Lee, H., Choe, S., Kim, S.-G., Michaels, S., & Lee, I. (2005). SUPPRESSOR OF FRIGIDA3 encodes a nuclear ACTIN-RELATED PROTEIN6 required for floral repression in Arabidopsis. *The Plant Cell*, *17*(10), 2647–2660. https://doi.org/10.1105/tpc.105.035485

Choi, K., Park, C., Lee, J., Oh, M., Noh, B., & Lee, I. (2007). Arabidopsis homologs of components of the SWR1 complex regulate flowering and plant development. *Development*, *134*(10), 1931–1941. https://doi.org/10.1242/dev.001891

Claeys, H., De Bodt, S., & Inzé, D. (2014). Gibberellins and DELLAs: Central nodes in growth regulatory networks. In *Trends in Plant Science* (Vol. 19, Issue 4, pp. 231–239). Elsevier Ltd. https://doi.org/10.1016/j.tplants.2013.10.001

Colebrook, E. H., Thomas, S. G., Phillips, A. L., & Hedden, P. (2014). The role of gibberellin signalling in plant responses to abiotic stress. In *Journal of Experimental Biology* (Vol. 217, Issue 1, pp. 67–75). Company of Biologists Ltd. https://doi.org/10.1242/jeb.089938

Coleman-Derr, D., & Zilberman, D. (2012). Deposition of Histone Variant H2A.Z within Gene Bodies Regulates Responsive Genes. *PLoS Genetics*, *8*(10). https://doi.org/10.1371/journal.pgen.1002988

Crevillén, P., Gómez-Zambrano, Á., López, J. A., Vázquez, J., Piñeiro, M., & Jarillo, J. A. (2019). Arabidopsis YAF9 histone readers modulate

flowering time through NuA4-complex-dependent H4 and H2A.Z histone acetylation at FLC chromatin. *New Phytologist*, *222*(4), 1893–1908. https://doi.org/10.1111/nph.15737

Dai, X., Bai, Y., Zhao, L., Dou, X., Liu, Y., Wang, L., Li, Y., Li, W., Hui, Y., Huang, X., Wang, Z., & Qin, Y. (2017a). H2A.Z Represses Gene Expression by Modulating Promoter Nucleosome Structure and Enhancer Histone Modifications in Arabidopsis. *Molecular Plant*, *10*(10), 1274–1292. https://doi.org/10.1016/J.MOLP.2017.09.007

Dai, X., Bai, Y., Zhao, L., Dou, X., Liu, Y., Wang, L., Li, Y., Li, W., Hui, Y., Huang, X., Wang, Z., & Qin, Y. (2017b). H2A.Z Represses Gene Expression by Modulating Promoter Nucleosome Structure and Enhancer Histone Modifications in Arabidopsis. *Molecular Plant*, *10*(10), 1274–1292. https://doi.org/10.1016/J.MOLP.2017.09.007

Davière, J. M., & Achard, P. (2016). A Pivotal Role of DELLAs in Regulating Multiple Hormone Signals. In *Molecular Plant* (Vol. 9, Issue 1, pp. 10–20). Elsevier. https://doi.org/10.1016/j.molp.2015.09.011

De Lucas, M., Davière, J. M., Rodríguez-Falcón, M., Pontin, M., Iglesias-Pedraz, J. M., Lorrain, S., Fankhauser, C., Blázquez, M. A., Titarenko, E., & Prat, S. (2008). A molecular framework for light and gibberellin control of cell elongation. *Nature*, *451*(7177), 480–484. https://doi.org/10.1038/nature06520

Deal, R. B. (2005). The Nuclear Actin-Related Protein ARP6 Is a Pleiotropic Developmental Regulator Required for the Maintenance of FLOWERING LOCUS C Expression and Repression of Flowering in Arabidopsis. *The Plant Cell*, *17*(10), 2633–2646. https://doi.org/10.1105/tpc.105.035196

Deal, R. B., Topp, C. N., McKinney, E. C., & Meagher, R. B. (2007). Repression of Flowering in Arabidopsis Requires Activation of FLOWERING LOCUS C Expression by the Histone Variant H2A.Z. *The Plant Cell*, *19*(1), 74–83. https://doi.org/10.1105/tpc.106.048447

Delgehyr, N., Wieland, U., Rangone, H., Pinson, X., Mao, G., Dzhindzhev, N. S., McLean, D., Riparbelli, M. G., Llamazares, S., Callaini, G., Gonzalez, C., & Glover, D. M. (2012). Drosophila Mgr, a prefoldin subunit cooperating with von Hippel Lindau to regulate tubulin stability. *Proceedings of the National Academy of Sciences*, *109*(15), 5729–5734. https://doi.org/10.1073/pnas.1108537109

Esteve-Bruna, D., Carrasco-López, C., Blanco-Touriñán, N., Iserte, J., Calleja-Cabrera, J., Perea-Resa, C., Úrbez, C., Carrasco, P., Yanovsky, M. J., Blázquez, M. A., Salinas, J., & Alabadí, D. (2020). Prefoldins contribute to maintaining the levels of the spliceosome LSM2-8 complex through Hsp90 in Arabidopsis. *Nucleic Acids Research*, *48*(11), 6280–6293. https://doi.org/10.1093/nar/gkaa354

Faast, R., Thonglairoam, V., Schulz, T. C., Beall, J., Wells, J. R. E., Taylor, H., Matthaei, K., Rathjen, P. D., Tremethick, D. J., & Lyons, I. (2001). Histone variant H2A.Z is required for early mammalian development. *Current Biology*, *11*, 1183–1187. https://doi.org/10.1016/S0960-9822(01)00329-3

Feng, S., Martinez, C., Gusmaroli, G., Wang, Y., Zhou, J., Wang, F., Chen, L., Yu, L., Iglesias-Pedraz, J. M., Kircher, S., Schäfer, E., Fu, X., Fan, L. M., & Deng, X. W. (2008). Coordinated regulation of Arabidopsis thaliana development by light and gibberellins. *Nature*, *451*(7177), 475–479. https://doi.org/10.1038/nature06448

Gallego-Bartolomé, J., Liu, W., Kuo, P. H., Feng, S., Ghoshal, B., Gardiner, J., Zhao, J. M. C., Park, S. Y., Chory, J., & Jacobsen, S. E. (2019). Co-targeting RNA Polymerases IV and V Promotes Efficient De Novo DNA Methylation in Arabidopsis. *Cell*, *176*(5), 1068-1082.e19. https://doi.org/10.1016/j.cell.2019.01.029

Galvão, V. C., Collani, S., Horrer, D., & Schmid, M. (2015). Gibberellic acid signaling is required for ambient temperature-mediated induction of flowering in Arabidopsis thaliana. *Plant Journal*, *84*(5), 949–962. https://doi.org/10.1111/tpj.13051

Geisler-Lee, J., O'Toole, N., Ammar, R., Provart, N. J., Millar, A. H., & Geisler, M. (2007). A predicted interactome for arabidopsis. *Plant Physiology*, *145*(2), 317–329. https://doi.org/10.1104/pp.107.103465

Geissler, S., Siegers, K., & Schiebel, E. (1998). A novel protein complex promoting formation of functional α- and γ-tubulin. *EMBO Journal*. https://doi.org/10.1093/emboj/17.4.952

Gerhold, C. B., & Gasser, S. M. (2014). INO80 and SWR complexes: Relating structure to function in chromatin remodeling. In *Trends in Cell Biology* (Vol. 24, Issue 11). https://doi.org/10.1016/j.tcb.2014.06.004

Gestaut, D., Roh, S. H., Ma, B., Pintilie, G., Joachimiak, L. A., Leitner, A., Walzthoeni, T., Aebersold, R., Chiu, W., & Frydman, J. (2019). The

Chaperonin TRiC/CCT Associates with Prefoldin through a Conserved Electrostatic Interface Essential for Cellular Proteostasis. *Cell*, *177*(3), 751-765.e15. https://doi.org/10.1016/j.cell.2019.03.012

Giaimo, B. D., Ferrante, F., Herchenröther, A., Hake, S. B., & Borggrefe, T. (2019). The histone variant H2A.Z in gene regulation. In *Epigenetics and Chromatin* (Vol. 12, Issue 1). BioMed Central Ltd. https://doi.org/10.1186/s13072-019-0274-9

Gómez-Zambrano, Á., Crevillén, P., Franco-Zorrilla, J. M., López, J. A., Moreno-Romero, J., Roszak, P., Santos-González, J., Jurado, S., Vázquez, J., Köhler, C., Solano, R., Piñeiro, M., & Jarillo, J. A. (2018). Arabidopsis SWC4 Binds DNA and Recruits the SWR1 Complex to Modulate Histone H2A.Z Deposition at Key Regulatory Genes. *Molecular Plant*, *11*(6), 815–832. https://doi.org/10.1016/j.molp.2018.03.014

Gómez-Zambrano, Á., Merini, W., & Calonje, M. (2019). The repressive role of Arabidopsis H2A.Z in transcriptional regulation depends on AtBMI1 activity. *Nature Communications*, *10*, 2828. https://doi.org/10.1038/s41467-019-10773-1

Gong, Y., Kakihara, Y., Krogan, N., Greenblatt, J., Emili, A., Zhang, Z., & Houry, W. A. (2009). An atlas of chaperone-protein interactions in Saccharomyces cerevisiae: Implications to protein folding pathways in the cell. *Molecular Systems Biology*, *5*, 275. https://doi.org/10.1038/msb.2009.26

Gu, Y., Deng, Z., Paredez, A. R., DeBolt, S., Wang, Z. Y., & Somerville, C. (2008). Prefoldin 6 is required for normal microtubule dynamics and organization in Arabidopsis. *Proceedings of the National Academy of Sciences of the United States of America*. https://doi.org/10.1073/pnas.0808652105

Guillemette, B., Bataille, A. R., Gévry, N., Adam, M., Blanchette, M., Robert, F., & Gaudreau, L. (2005). Variant histone H2A.z is globally localized to the promoters of inactive yeast genes and regulates nucleosome positioning. *PLoS Biology*, *3*(12), 1–11. https://doi.org/10.1371/journal.pbio.0030384

Hagio, Y., Kimura, Y., Taira, T., Fujioka, Y., Iguchi-Ariga, S. M. M., & Ariga, H. (2006). Distinct localizations and repression activities of MM-1 isoforms toward c-Myc. *Journal of Cellular Biochemistry*, *97*(1), 145–155. https://doi.org/10.1002/jcb.20619

Hedden, P., & Thomas, S. G. (2012). Gibberellin biosynthesis and its regulation. In *Biochemical Journal* (Vol. 444, Issue 1, pp. 11–25). https://doi.org/10.1042/BJ20120245

Hernández-García, J., Briones-Moreno, A., Dumas, R., & Blázquez, M. A. (2019). Origin of Gibberellin-Dependent Transcriptional Regulation by Molecular Exploitation of a Transactivation Domain in della Proteins. *Molecular Biology and Evolution*, *36*(5), 908–918. https://doi.org/10.1093/molbev/msz009

Hou, X., Lee, L. Y. C., Xia, K., Yan, Y., & Yu, H. (2010). DELLAs Modulate Jasmonate Signaling via Competitive Binding to JAZs. *Developmental Cell*, *19*(6), 884–894. https://doi.org/10.1016/j.devcel.2010.10.024

Hu, Y., Comjean, A., Perrimon, N., & Mohr, S. E. (2017). The Drosophila Gene Expression Tool (DGET) for expression analyses. *BMC Bioinformatics*, *18*(1). https://doi.org/10.1186/s12859-017-1509-z

Huang, W., Loganantharaj, R., Schroeder, B., Fargo, D., & Li, L. (2013). PAVIS: A tool for Peak Annotation and Visualization. *Bioinformatics*, *29*(23), 3097–3099. https://doi.org/10.1093/bioinformatics/btt520

Jackson, J. D., & Gorovsky, M. A. (2000). Histone H2A.Z has a conserved function that is distinct from that of the major H2A sequence variants. *Nucleic Acids Research*, *28*(19), 3811–3816. https://doi.org/10.1093/nar/28.19.3811

Jarillo, J. A., & Piñeiro, M. (2015). H2A.Z mediates different aspects of chromatin function and modulates flowering responses in Arabidopsis. *Plant Journal*, *83*(1), 96–109. https://doi.org/10.1111/tpj.12873

Kapoor, P., & Shen, X. (2014). Mechanisms of nuclear actin in chromatin-remodeling complexes. In *Trends in Cell Biology* (Vol. 24, Issue 4, pp. 238–246). https://doi.org/10.1016/j.tcb.2013.10.007

Keogh, M. C., Mennella, T. A., Sawa, C., Berthelet, S., Krogan, N. J., Wolek, A., Podolny, V., Carpenter, L. R., Greenblatt, J. F., Baetz, K., & Buratowski, S. (2006). The Saccharomyces cerevisiae histone H2A variant Htz1 is acetylated by NuA4. *Genes and Development*. https://doi.org/10.1101/gad.1388106

Kim, H., Shin, J., Kim, E., Kim, H., Hwang, S., Shim, J. E., & Lee, I. (2014). YeastNet v3: A public database of data-specific and integrated functional gene networks for Saccharomyces cerevisiae. *Nucleic Acids Research*, *42*(D1). https://doi.org/10.1093/nar/gkt981

Kim, S. Y., Kim, J. C., Kim, J. K., Kim, H. J., Lee, H. M., Choi, M. S., Maeng, P. J., & Ahn, J. K. (2008). Hepatitis B virus X protein enhances NFkappaB activity through cooperating with VBP1. *BMB Reports*, *41*(2), 158–163. http://www.ncbi.nlm.nih.gov/pubmed/18315953

Kimura, Y., Nagao, A., Fujioka, Y., Satou, A., Taira, T., Iguchi-Ariga, S. M. M., & Ariga, H. (2007). MM-1 facilitates degradation of c-Myc by recruiting proteasome and a novel ubiquitin E3 ligase. *International Journal of Oncology*. https://doi.org/10.3892/ijo.31.4.829

Kobor, M. S., Venkatasubrahmanyam, S., Meneghini, M. D., Gin, J. W., Jennings, J. L., Link, A. J., Madhani, H. D., & Rine, J. (2004). A protein complex containing the conserved Swi2/Snf2-related ATPase Swr1p deposits histone variant H2A.Z into euchromatin. *PLoS Biology*, *2*(5), E131. https://doi.org/10.1371/journal.pbio.0020131

Kolde, R. (2015). pheatmap : Pretty Heatmaps. In *R package version 1.0.8* (pp. 1–7). https://cran.r-project.org/web/packages/pheatmap/pheatmap.pdf

Krogan, N. J., Keogh, M. C., Datta, N., Sawa, C., Ryan, O. W., Ding, H., Haw, R. A., Pootoolal, J., Tong, A., Canadien, V., Richards, D. P., Wu, X., Emili, A., Hughes, T. R., Buratowski, S., & Greenblatt, J. F. (2003). A Snf2 Family ATPase Complex Required for Recruitment of the Histone H2A Variant Htz1. *Molecular Cell*, *12*(6), 1565–1576. https://doi.org/10.1016/S1097-2765(03)00497-0

Kulkarni, S. R., Vaneechoutte, D., Van de Velde, J., & Vandepoele, K. (2018). TF2Network: predicting transcription factor regulators and gene regulatory networks in Arabidopsis using publicly available binding site information. *Nucleic Acids Research*, *46*(6), e31. https://doi.org/10.1093/nar/gkx1279

Kumar, S. V., Lucyshyn, D., Jaeger, K. E., Alós, E., Alvey, E., Harberd, N. P., & Wigge, P. A. (2012). Transcription factor PIF4 controls the thermosensory activation of flowering. *Nature*, *484*(7393), 242–245. https://doi.org/10.1038/nature10928

Kumar, S. V., & Wigge, P. A. (2010). H2A.Z-Containing Nucleosomes Mediate the Thermosensory Response in Arabidopsis. *Cell*, *140*(1), 136–147. https://doi.org/10.1016/j.cell.2009.11.006

Lacefield, S., Magendantz, M., & Solomon, F. (2006). Consequences of defective tubulin folding on heterodimer levels, mitosis and spindle

morphology in Saccharomyces cerevisiae. *Genetics*. https://doi.org/10.1534/genetics.105.055160

Langmead, B., & Salzberg, S. L. (2012). Fast gapped-read alignment with Bowtie 2. *Nature Methods*, *9*(4), 357–359. https://doi.org/10.1038/nmeth.1923

Lázaro, A., Gómez-Zambrano, Á., López-González, L., Piñeiro, M., & Jarillo, J. A. (2008). Mutations in the Arabidopsis SWC6 gene, encoding a component of the SWR1 chromatin remodelling complex, accelerate flowering time and alter leaf and flower development. *Journal of Experimental Botany*, *59*(3), 653–666. https://doi.org/10.1093/jxb/erm332

Lee, Y. S., Smith, R. S., Jordan, W., King, B. L., Won, J., Valpuesta, J. M., Naggert, J. K., & Nishina, P. M. (2011). Prefoldin 5 is required for normal sensory and neuronal development in a murine model. *Journal of Biological Chemistry*, *286*(1), 726–736. https://doi.org/10.1074/jbc.M110.177352

Leroux, M. R. (1999). MtGimC, a novel archaeal chaperone related to the eukaryotic chaperonin cofactor GimC/prefoldin. *The EMBO Journal*. https://doi.org/10.1093/emboj/18.23.6730

Lim, S., Glover, D. J., & Clark, D. S. (2018). Prefoldins in Archaea. *Advances in Experimental Medicine and Biology*, *1106*, 11–23. https://doi.org/10.1007/978-3-030-00737-9_2

Liu, X., & Gorovsky, M. A. (1996). Cloning and characterization of the major histone H2A genes completes the cloning and sequencing of known histone genes of Tetrahymena thermophila. *Nucleic Acids Research*, *24*(15), 3023–3030. https://doi.org/10.1093/nar/24.15.3023

Locascio, A., Blázquez, M. A., & Alabadí, D. (2013). Dynamic regulation of cortical microtubule organization through prefoldin-DELLA interaction. *Current Biology*. https://doi.org/10.1016/j.cub.2013.03.053

Lu, P. Y. T., Lévesque, N., & Kobor, M. S. (2009). NuA4 and SWR1-C: Two chromatin-modifying complexes with overlapping functions and components. *Biochemistry and Cell Biology*, *87*(5), 799–815. https://doi.org/10.1139/O09-062

Luger, K., Mäder, A. W., Richmond, R. K., Sargent, D. F., & Richmond, T. J. (1997). Crystal structure of the nucleosome core particle at 2.8 Å resolution. *Nature*, *389*(6648), 251–260. https://doi.org/10.1038/38444

Lundin, V. F., Srayko, M., Hyman, A. A., & Leroux, M. R. (2008). Efficient chaperone-mediated tubulin biogenesis is essential for cell division and cell migration in C. elegans. *Developmental Biology*. https://doi.org/10.1016/j.ydbio.2007.10.022

Luo, Y., Hou, X., Zhang, C., Tan, L., Shao, C., Lin, R., Su, Y., Cai, X., Li, L., Chen, S., & He, X. (2020). A plant-specific SWR1 chromatin-remodeling complex couples histone H2A.Z deposition with nucleosome sliding. *The EMBO Journal*, *39*(7). https://doi.org/10.15252/embj.2019102008

Malik, H. S., & Henikoff, S. (2003). Phylogenomics of the nucleosome. *Nature Structural Biology*, *10*(11), 882–891. https://doi.org/10.1038/nsb996

March-Díaz, R., García-Domínguez, M., Lozano-Juste, J., León, J., Florencio, F. J., & Reyes, J. C. (2008). Histone H2A.Z and homologues of components of the SWR1 complex are required to control immunity in Arabidopsis. *Plant Journal*, *53*(3), 475–487. https://doi.org/10.1111/j.1365-313X.2007.03361.x

March-Díaz, R., & Reyes, J. C. (2009). The beauty of being a variant: H2A.Z and the SWR1 complex in plants. *Molecular Plant*, *2*(4), 565–577. https://doi.org/10.1093/mp/ssp019

Marín-de la Rosa, N., Pfeiffer, A., Hill, K., Locascio, A., Bhalerao, R. P., Miskolczi, P., Grønlund, A. L., Wanchoo-Kohli, A., Thomas, S. G., Bennett, M. J., Lohmann, J. U., Blázquez, M. A., & Alabadí, D. (2015). Genome Wide Binding Site Analysis Reveals Transcriptional Coactivation of Cytokinin-Responsive Genes by DELLA Proteins. *PLoS Genetics*, *11*(7), e1005337. https://doi.org/10.1371/journal.pgen.1005337

Marín-de La Rosa, N., Sotillo, B., Miskolczi, P., Gibbs, D. J., Vicente, J., Carbonero, P., Oñate-Sánchez, L., Holdsworth, M. J., Bhalerao, R., Alabadí, D., & Blázquez, M. A. (2014). Large-scale identification of gibberellin-related transcription factors defines group VII ETHYLENE RESPONSE FACTORS as functional DELLA partners. *Plant Physiology*, *166*(2), 1022–1032. https://doi.org/10.1104/pp.114.244723

Marques, M., Laflamme, L., Gervais, A. L., & Gaudreau, L. (2010). Reconciling the positive and negative roles of histone H2A.Z in gene transcription. *Epigenetics*, *5*(4), 267–272. https://doi.org/10.4161/epi.5.4.11520

Martín-Benito, J., Boskovic, J., Gómez-Puertas, P., Carrascosa, J. L., Simons, C. T., Lewis, S. A., Bartolini, F., Cowan, N. J., & Valpuesta, J. M. (2002). Structure of eukaryotic prefoldin and of its complexes with unfolded actin and the cytosolic chaperonin CCT. *EMBO Journal*, *21*(23), 6377–6386. https://doi.org/10.1093/emboj/cdf640

Martin-Trillo, M., Lázaro, A., Scott Poethig, R., Gómez-Mena, C., Piñeiro, M. A., Martinez-Zapater, J. M., & Jarillo, J. A. (2006). Early in short days 1 (ESD1) encodes Actin-Related Protein 6 (AtARP6), a putative component of chromatin remodelling complexes that positively regulates FLC accumulation in Arabidopsis. *Development*, *133*(7), 1241–1252. https://doi.org/10.1242/dev.02301

McCarthy, D. J., Chen, Y., & Smyth, G. K. (2012). Differential expression analysis of multifactor RNA-Seq experiments with respect to biological variation. *Nucleic Acids Research*, *40*(10), 4288–4297. https://doi.org/10.1093/nar/gks042

Millán-Zambrano, G., & Chávez, S. (2014). Nuclear functions of prefoldin. *Open Biology*, *4*, 140085. https://doi.org/10.1098/rsob.140085

Millán-Zambrano, G., Rodríguez-Gil, A., Peñate, X., de Miguel-Jiménez, L., Morillo-Huesca, M., Krogan, N., & Chávez, S. (2013). The Prefoldin Complex Regulates Chromatin Dynamics during Transcription Elongation. *PLoS Genetics*, *9*(9). https://doi.org/10.1371/journal.pgen.1003776

Mizuguchi, G., Shen, X., Landry, J., Wu, W. H., Sen, S., & Wu, C. (2004). ATP-Driven Exchange of Histone H2AZ Variant Catalyzed by SWR1 Chromatin Remodeling Complex. *Science*, *303*(5656), 343–348. https://doi.org/10.1126/science.1090701

Mori, K., Maeda, Y., Kitaura, H., Taira, T., Iguchi-Ariga, S. M. M., & Ariga, H. (1998). MM-1, a novel c-Myc-associating protein that represses transcriptional activity of c-Myc. *Journal of Biological Chemistry*. https://doi.org/10.1074/jbc.273.45.29794

Morrison, A. J., & Shen, X. (2009). Chromatin remodelling beyond transcription: The INO80 and SWR1 complexes. In *Nature Reviews Molecular Cell Biology* (Vol. 10, Issue 6, pp. 373–384). https://doi.org/10.1038/nrm2693

Narita, R., Kitaura, H., Torii, A., Tashiro, E., Miyazawa, M., Ariga, H., & Iguchi-Ariga, S. M. M. (2012). Rabring7 degrades c-Myc through

complex formation with MM-1. *PLoS ONE*. https://doi.org/10.1371/journal.pone.0041891

Nguyen, V. Q., Ranjan, A., Stengel, F., Wei, D., Aebersold, R., Wu, C., & Leschziner, A. E. (2013). Molecular architecture of the ATP-dependent chromatin-remodeling complex SWR1. *Cell*, *154*(6), 1220–1231. https://doi.org/10.1016/j.cell.2013.08.018

Noh, Y. S., & Amasino, R. M. (2003). PIE1, an ISWI family gene, is required for FLC activation and floral repression in Arabidopsis. *Plant Cell*, *15*(7), 1671–1682. https://doi.org/10.1105/tpc.012161

Papamichos-Chronakis, M., Watanabe, S., Rando, O. J., & Peterson, C. L. (2011). Global regulation of H2A.Z localization by the INO80 chromatin-remodeling enzyme is essential for genome integrity. *Cell*, *144*(2), 200–213. https://doi.org/10.1016/j.cell.2010.12.021

Payán-Bravo, L., Peñate, X., & Chávez, S. (2018). Functional Contributions of Prefoldin to Gene Expression. In N. Djouder (Ed.), *Prefoldins: the new chaperones* (pp. 1–10). Springer International Publishing. https://doi.org/10.1007/978-3-030-00737-9_1

Perea-Resa, C., Rodríguez-Milla, M. A., Iniesto, E., Rubio, V., & Salinas, J. (2017). Prefoldins Negatively Regulate Cold Acclimation in Arabidopsis thaliana by Promoting Nuclear Proteasome-Mediated HY5 Degradation. *Molecular Plant*, *10*(6), 791–804. https://doi.org/10.1016/j.molp.2017.03.012

Potok, M. E., Wang, Y., Xu, L., Zhong, Z., Liu, W., Feng, S., Naranbaatar, B., Rayatpisheh, S., Wang, Z., Wohlschlegel, J. A., Ausin, I., & Jacobsen, S. E. (2019). Arabidopsis SWR1-associated protein methyl-CpG-binding domain 9 is required for histone H2A.Z deposition. *Nature Communications*, *10*(1), 3352. https://doi.org/10.1038/s41467-019-11291-w

Rodríguez-Milla, M. A., & Salinas, J. (2009). Prefoldins 3 and 5 play an essential role in Arabidopsis tolerance to salt stress. *Molecular Plant*, *2*(3), 526–534. https://doi.org/10.1093/mp/ssp016

Rueden, C. T., Schindelin, J., Hiner, M. C., DeZonia, B. E., Walter, A. E., Arena, E. T., & Eliceiri, K. W. (2017). ImageJ2: ImageJ for the next generation of scientific image data. *BMC Bioinformatics*, *18*(1). https://doi.org/10.1186/s12859-017-1934-z

Satou, A., Taira, T., Iguchi-Ariga, S. M. M., & Ariga, H. (2001). A novel

transrepression pathway of c-Myc: Recruitment of a transcriptional corepressor complex to c-Myc by MM-1, a c-Myc-binding protein. *Journal of Biological Chemistry*. https://doi.org/10.1074/jbc.M104937200

Scheres, B., & Van Der Putten, W. H. (2017). The plant perceptron connects environment to development. In *Nature* (Vol. 543, Issue 7645, pp. 337–345). Nature Publishing Group. https://doi.org/10.1038/nature22010

Shannon, P., Markiel, A., Ozier, O., Baliga, N. S., Wang, J. T., Ramage, D., Amin, N., Schwikowski, B., & Ideker, T. (2003). Cytoscape: A software Environment for integrated models of biomolecular interaction networks. *Genome Research*, *13*(11), 2498–2504. https://doi.org/10.1101/gr.1239303

Shen, X., Mizuguchi, G., Hamiche, A., & Carl, W. (2000). A chromatin remodelling complex involved in transcription and DNA processing. *Nature*, *406*, 541–544. https://doi.org/10.1038/35020123

Siegert, R., Leroux, M. R., Scheufler, C., Hartl, F. U., & Moarefi, I. (2000). Structure of the molecular chaperone prefoldin: Unique interaction of multiple coiled coil tentacles with unfolded proteins. *Cell*. https://doi.org/10.1016/S0092-8674(00)00165-3

Sijacic, P., Holder, D. H., Bajic, M., & Deal, R. B. (2019). Methyl-CpG-binding domain 9 (MBD9) is required for H2A.Z incorporation into chromatin at a subset of H2A.Z-enriched regions in the Arabidopsis genome. *PLoS Genetics*, *15*(8), e1008326. https://doi.org/10.1371/journal.pgen.1008326

Smith, A. P., Jain, A., Deal, R. B., Nagarajan, V. K., Poling, M. D., Raghothama, K. G., & Meagher, R. B. (2010). Histone H2A.Z Regulates the Expression of Several Classes of Phosphate Starvation Response Genes But Not as a Transcriptional Activator. *Plant Physiology*, *152*(1), 217–225. https://doi.org/10.1104/pp.109.145532

Sörgjerd, K. M., Zako, T., Sakono, M., Stirling, P. C., Leroux, M. R., Saito, T., Nilsson, P., Sekimoto, M., Saido, T. C., & Maeda, M. (2013). Human prefoldin inhibits amyloid-β (Aβ) fibrillation and contributes to formation of nontoxic Aβ aggregates. *Biochemistry*. https://doi.org/10.1021/bi301705c

Stempor, P., & Ahringer, J. (2016). SeqPlots - Interactive software for exploratory data analyses, pattern discovery and visualization in genomics. *Wellcome Open Research*, *1*.

https://doi.org/10.12688/wellcomeopenres.10004.1

Subramanian, V., Fields, P. A., & Boyer, L. A. (2015). H2A.Z: A molecular rheostat for transcriptional control. *F1000Prime Reports*, *7*. https://doi.org/10.12703/P7-01

Sura, W., Kabza, M., Karlowski, W. M., Bieluszewski, T., Kus-Slowinska, M., Pawełoszek, Ł., Sadowski, J., & Ziolkowski, P. A. (2017). Dual Role of the Histone Variant H2A.Z in Transcriptional Regulation of Stress-Response Genes. *The Plant Cell*, *29*(4), 791–807. https://doi.org/10.1105/tpc.16.00573

Takano, M., Tashiro, E., Kitamura, A., Maita, H., Iguchi-Ariga, S. M. M., Kinjo, M., & Ariga, H. (2014). Prefoldin prevents aggregation of α-synuclein. *Brain Research*. https://doi.org/10.1016/j.brainres.2013.10.034

Talbert, P. B., & Henikoff, S. (2010). Histone variants ancient wrap artists of the epigenome. In *Nature Reviews Molecular Cell Biology* (Vol. 11, Issue 4, pp. 264–275). https://doi.org/10.1038/nrm2861

Talbert, P. B., & Henikoff, S. (2014). Environmental responses mediated by histone variants. *Trends in Cell Biology*, *24*(11), 642–650. https://doi.org/10.1016/j.tcb.2014.07.006

Tashiro, E., Zako, T., Muto, H., Itoo, Y., Sörgjerd, K., Terada, N., Abe, A., Miyazawa, M., Kitamura, A., Kitaura, H., Kubota, H., Maeda, M., Momoi, T., Iguchi-Ariga, S. M. M., Kinjo, M., & Ariga, H. (2013). Prefoldin protects neuronal cells from polyglutamine toxicity by preventing aggregation formation. *Journal of Biological Chemistry*. https://doi.org/10.1074/jbc.M113.477984

Thatcher, T. H., & Gorovsky, M. A. (1994). Phylogenetic analysis of the core histones H2A, H2B, H3, and H4. *Nucleic Acids Research*, *22*(2), 174–179. https://doi.org/10.1093/nar/22.2.174

Thomas, S. G., Blázquez, M. A., & Alabadí, D. (2016). Della Proteins: Master Regulators of Gibberellin-Responsive Growth and Development. In *Annual Plant Reviews: The Gibberellins* (Vol. 49, pp. 189–228). https://doi.org/10.1002/9781119210436.ch7

Vainberg, I. E., Lewis, S. A., Rommelaere, H., Ampe, C., Vandekerckhove, J., Klein, H. L., & Cowan, N. J. (1998). Prefoldin, a chaperone that delivers unfolded proteins to cytosolic chaperonin. *Cell*. https://doi.org/10.1016/S0092-8674(00)81446-4

Van Daal, A., & Elgin, S. C. R. (1992). Histone variant, H2AvD, is essential Drosophila melanogaster. *Molecular Biology of the Cell*, *3*, 593–602. https://doi.org/10.1091/mbc.3.6.593

Vera-Sirera, F., Gomez, M. D., & Perez-Amador, M. A. (2016). DELLA Proteins, a Group of GRAS Transcription Regulators that Mediate Gibberellin Signaling. In *Plant Transcription Factors: Evolutionary, Structural and Functional Aspects* (pp. 313–328). Elsevier Inc. https://doi.org/10.1016/B978-0-12-800854-6.00020-8

Wang, D., Shi, W., Tang, Y., Liu, Y., He, K., Hu, Y., Li, J., Yang, Y., & Song, J. (2017). Prefoldin 1 promotes EMT and lung cancer progression by suppressing cyclin A expression. *Oncogene*, *36*(7), 885–898. https://doi.org/10.1038/onc.2016.257

Watanabe, K. I., Ozaki, T., Nakagawa, T., Miyazaki, K., Takahashi, M., Hosoda, M., Hayashi, S., Todo, S., & Nakagawara, A. (2002). Physical interaction of p73 with c-Myc and MM1, a c-Myc-binding protein, and modulation of the p73 function. *Journal of Biological Chemistry*, *277*(17), 15113–15123. https://doi.org/10.1074/jbc.M111281200

Wu, W. H., Alami, S., Luk, E., Wu, C. H., Sen, S., Mizuguchi, G., Wei, D., & Wu, C. (2005). Swc2 is a widely conserved H2AZ-binding module essential for ATP-dependent histone exchange. *Nature Structural and Molecular Biology*, *12*(12), 1064–1071. https://doi.org/10.1038/nsmb1023

Wu, W. H., Wu, C. H., Ladurner, A., Mizuguchi, G., Wei, D., Xiao, H., Luk, E., Ranjant, A., & Wu, C. (2009). N terminus of Swr1 binds to histone H2AZ and provides a platform for subunit assembly in the chromatin remodeling complex. *Journal of Biological Chemistry*, *284*(10), 6200–6207. https://doi.org/10.1074/jbc.M808830200

Yamane, T., Shimizu, T., Takahashi-Niki, K., Takekoshi, Y., Iguchi-Ariga, S. M. M., & Ariga, H. (2015). Deficiency of spermatogenesis and reduced expression of spermatogenesis-related genes in prefoldin 5-mutant mice. *Biochemistry and Biophysics Reports*, *1*(1), 52–61. https://doi.org/10.1016/j.bbrep.2015.03.005

Yang, D. L., Yao, J., Mei, C. S., Tong, X. H., Zeng, L. J., Li, Q., Xiao, L. T., Sun, T. P., Li, J., Deng, X. W., Lee, C. M., Thomashow, M. F., Yang, Y., He, Z., & He, S. Y. (2012). Plant hormone jasmonate prioritizes defense over growth by interfering with gibberellin signaling cascade. *Proceedings of the National Academy of Sciences of the United States of America*, *109*(19),

1192–1200. https://doi.org/10.1073/pnas.1201616109

Yang, H., Howard, M., & Dean, C. (2014). Antagonistic roles for H3K36me3 and H3K27me3 in the cold-induced epigenetic switch at Arabidopsis FLC. *Current Biology*, *24*(15), 1793–1797. https://doi.org/10.1016/j.cub.2014.06.047

Yelagandula, R., Stroud, H., Holec, S., Zhou, K., Feng, S., Zhong, X., Muthurajan, U. M., Nie, X., Kawashima, T., Groth, M., Luger, K., Jacobsen, S. E., & Berger, F. (2014). The histone variant H2A.W defines heterochromatin and promotes chromatin condensation in arabidopsis. *Cell*, *158*(1), 98–109. https://doi.org/10.1016/j.cell.2014.06.006

Yi, H., Sardesai, N., Fujinuma, T., Chan, C.-W., Veena, & Gelvin, S. B. (2006). Constitutive expression exposes functional redundancy between the Arabidopsis histone H2A gene HTA1 and other H2A gene family members. *The Plant Cell*, *18*(7), 1575–1589. https://doi.org/10.1105/tpc.105.039719

Yoshida, T., Kitaura, H., Hagio, Y., Sato, T., Iguchi-Ariga, S. M. M., & Ariga, H. (2008). Negative regulation of the Wnt signal by MM-1 through inhibiting expression of the wnt4 gene. *Experimental Cell Research*. https://doi.org/10.1016/j.yexcr.2008.01.002

Yu, G., Li, F., Qin, Y., Bo, X., Wu, Y., & Wang, S. (2010). GOSemSim: An R package for measuring semantic similarity among GO terms and gene products. *Bioinformatics*, *26*(7), 976–978. https://doi.org/10.1093/bioinformatics/btq064

Yu, G., Wang, L. G., Han, Y., & He, Q. Y. (2012). ClusterProfiler: An R package for comparing biological themes among gene clusters. *OMICS A Journal of Integrative Biology*, *16*(5), 284–287. https://doi.org/10.1089/omi.2011.0118

Zang, C., Schones, D. E., Zeng, C., Cui, K., Zhao, K., & Peng, W. (2009). A clustering approach for identification of enriched domains from histone modification ChIP-Seq data. *Bioinformatics*, *25*(15), 1952–1958. https://doi.org/10.1093/bioinformatics/btp340

Zhang, H., Tang, K., Qian, W., Duan, C. G., Wang, B., Zhang, H., Wang, P., Zhu, X., Lang, Z., Yang, Y., & Zhu, J. K. (2014). An Rrp6-like Protein Positively Regulates Noncoding RNA Levels and DNA Methylation in Arabidopsis. *Molecular Cell*, *54*(3), 418–430. https://doi.org/10.1016/j.molcel.2014.03.019

Zhang, Z., & Pugh, B. F. (2011). Genomic organization of H2Av containing nucleosomes in Drosophila heterochromatin. *PLoS ONE*, *6*(6). https://doi.org/10.1371/journal.pone.0020511

Zilberman, D., Coleman-Derr, D., Ballinger, T., & Henikoff, S. (2008). Histone H2A.Z and DNA methylation are mutually antagonistic chromatin marks. *Nature*, *456*(7218), 125–129. https://doi.org/10.1038/nature07324